Table 3. Preparation of the Biotinylated PEG Tethered Chain Surface with Underbrushed PEG

surface	SPR response (deg) PEG2k	PEG5k	biotin[f]	density (ng/cm²) PEG[e]	Biotin[g]
PEG2–b	0.130 ± 0.018[a]	0	0.015 ± 0.002	199 ± 28	15 ± 2
PEG2k-b/5k	0.130 ± 0.018[a]	0.090 ± 0.010[d]	0.015 ± 0.002	337 ± 43	15 ± 2
PEG5k-b	0	0.180 ± 0.012[b]	0.014 ± 0.002	276 ± 18	15 ± 2
PEG5k-b/2k	0.090 ± 0.015[c]	0.180 ± 0.012[b]	0.014 ± 0.002	414 ± 41	15 ± 2

[a] The first PEG modification was carried out with the 1.0 mg/mL PEG2k solution for 15–20 min (20 μL/min) to adjust the immobilized amount to 0.13–0.18. [b] The same as (*a*) using PEG5k. [c] Twice repetitive backfilling modifications were carried out using PEG2k (1.0 mg/mL PEG solution for 20 min (20μL/min). [d] The same as (*c*) using PEG5K. [e] The PEG adlayer density was calculated from the total SPR angle shift according to refs 37 and 38. [f] Biotin modification was carried out under the conditions of 0.7 mg/mL biocytin hydrazide solution for 20–25 min (20 μL/min). [g] The biotin density was calculated from the SPR angle shift according to refs 4 and 14 (n = 4, ±SEM).

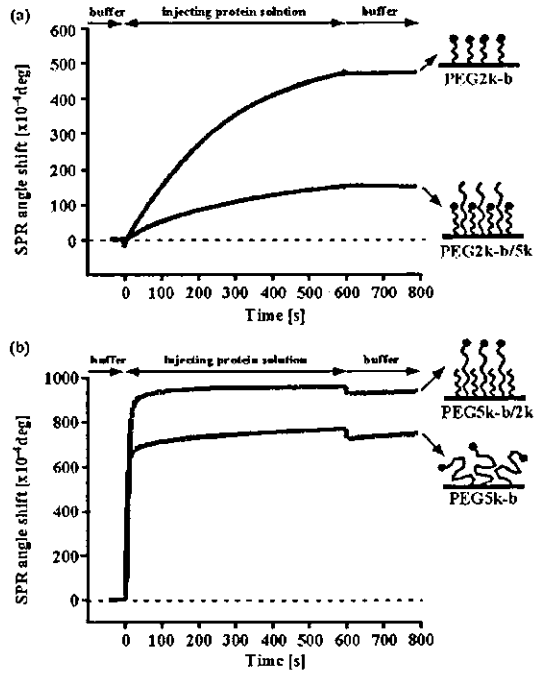

Figure 3. SPR sensorgrams for the binding of streptavidin on the biotinylated PEG surface filled with nonbiotinylated PEG of varying molecular weight: (a) PEG2k-b and PEG2k-b/5k surfaces and (b) PEG5k-band PEG5k-b/2k surfaces, using 10 μg/mL streptavidin at a flow rate of 20 μL/min for 10 min at 25 °C. The conditions of PEGylated surfaces with biotin moieties were described in Table 3.

the surface tethered with the longer biotin-installed PEG chain revealed an improved streptavidin binding through a further treatment with a shorter PEG chain. This increased accessibility of streptavidin molecule to the biotinylated PEG5k chain end with the underbrushed layer of PEG2k may be explained by the more elongated conformation of PEG5k than that of sole PEG5k brushes due to the presence of underbrushed PEG2k layer.

In conclusion, a reactive PEG layer was constructed on a gold sensor surface for SPR measurement using α-acetal-ω-mercapto-PEG with a precisely modulated molecular weight. After the treatment with PEG having a molecular weight of 5000, a shorter PEG (2000) was introduced onto the sensor chip for SPR measurement. The mixed PEG chain-tethered surface thus constructed showed an almost complete nonfouling character. The mixed PEG surface possessing a ligand molecule at the PEG chain end showed high sensing ability, avoiding nonspecific adsorption of coexisting biocompounds and recognizing only biomolecules that had a specific affinity for the ligand molecule. Shorter PEG, viz. an underbrushed PEG layer to increase the PEG surface density, played a substantial role in minimizing nonspecific adsorption and achieving specific biosensing with a very high S/N ratio. These results represent significant advances toward the expansion of SPR biosensing to a wider range of biochemical interactions.

ACKNOWLEDGMENT

Part of this work was financially supported by the Japan Science and Technology Corporation (JST).

SUPPORTING INFORMATION AVAILABLE

Additional information as noted in text. This material is available free of charge via the Internet at http://pubs.acs.org.

Received for review September 19, 2004. Accepted November 28, 2004.

AC0486140

J|A|C|S
COMMUNICATIONS

Published on Web 02/11/2005

PEGylated Polyplex Micelles from Triblock Catiomers with Spatially Ordered Layering of Condensed pDNA and Buffering Units for Enhanced Intracellular Gene Delivery

Shigeto Fukushima,[†,§] Kanjiro Miyata,[†,#] Nobuhiro Nishiyama,[*,‡] Naoki Kanayama,[†,#] Yuichi Yamasaki,[†,#] and Kazunori Kataoka*[,†,‡,#]

Department of Materials Science and Engineering, Graduate School of Engineering, The University of Tokyo, 7-3-1 Hongo, Bunkyo-ku, Tokyo 113-8656, Japan, Center for Disease Biology and Integrative Medicine, Graduate School of Medicine, The University of Tokyo, Tokyo 113-0033, Japan, Nippon Kayaku Co., Ltd., and CREST, Japan Science and Technology Agency, Japan

Received September 29, 2004; E-mail: nishiyama@bmw.t.u-tokyo.ac.jp; kataoka@bmw.t.u-tokyo.ac.jp

Successful in vivo gene therapy relies on the development of efficient gene vectors. Especially, the synthetic vectors based on cationic polymers have been attracting much attention because of their safety for clinical application and the variety of their chemical design. Nevertheless, the rational design of synthetic vectors remains to be established. Many previous studies have described that polyplexes formed from polycations with a comparatively low pK_a values, such as polyethylenimine (PEI), show a high transfection activity,[1] which has been explained by the proton sponge effect.[2] However, such polycations have a weak affinity to DNA, resulting in the formation of polyplexes that are easily dissociated under physiological conditions. Also, the buffer capacity of polycations may be hampered by their facilitated protonation due to the zipper effect or the neighboring group effect during the complexation process with DNA.[3] These problems could be modulated by the addition of excess polycations (i.e., increasing the N/P ratios[4]) to form polyplexes with a cationically deviated composition. However, it was recently demonstrated that free polycations in such polyplexes substantially contribute to efficient transfection but also mediate toxic effects. Hence, polyplex systems useful for in vivo gene delivery are required to achieve efficient transfection under the condition without free polycations.[5] Also, the gene delivery systems need to be equipped with high stability and biocompatibility. Here, A−B−C type triblock copolymers consisting of three distinctive functional segments were newly designed for constructing gene delivery systems which might not require free polycations to achieve enhanced gene expression but might provide a high stability and biocompatibility. In the present design of triblock copolymers, poly(ethylene glycol) (PEG) was used as the biocompatible A-segment, poly[(3-morpholinopropyl) aspartamide] (PMPA) was used as the low-pK_a B-segment with a buffering capacity, and poly(L-lysine) (PLL) was used as the high-pK_a C-segment to condense the DNA (Figure 1).

The triblock copolymer, PEG−PMPA−PLL, was synthesized by the successive ring-opening polymerization of the *N*-carboxyanhydrides (NCAs) of β-benzyl-L-aspartate (BLA) and ϵ-(benzyloxycarbonyl)-L-lysine (Lys(Z)), initiated by the $-NH_2$ group of α-methoxy-ω-amino PEG (MW 12 000), followed by the aminolysis of the benzyl ester of PBLA using 4-(3-aminopropyl)morpholine and the deprotection of the Z groups of PLL(Z).[6] The triblock copolymer was confirmed to have a narrow molecular weight distribution (M_w/M_n = 1.18), and the number of repeating units of

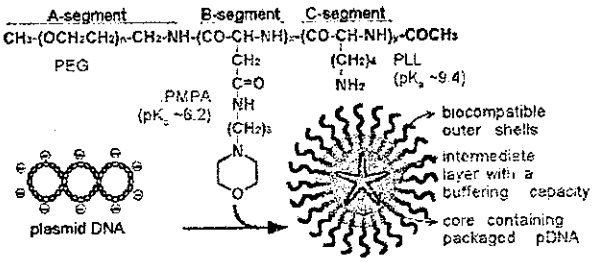

Figure 1. Chemical structure of PEG−PMPA−PLL triblock copolymers and schematic illustration of the hypothesized three-layered polyplex micelles with spatially regulated structure.

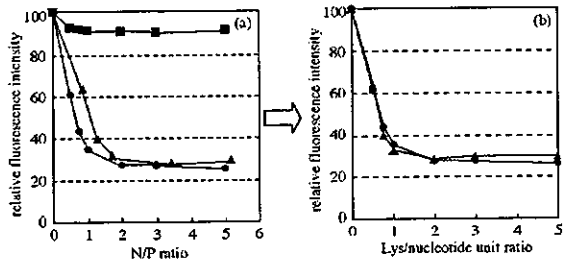

Figure 2. Interaction of PEG−PLL (circle), PEG−PMPA (square), and PEG−PMPA−PLL (triangle) copolymers with pDNA in 10 mM PBS (pH 7.4) + 150 mM NaCl, evaluated by dye exclusion assay. (a) In this figure, the *X*-axis represents the N/P ratio, where N stands for the total of MPA and Lys units. (b) In this figure, the *X* axis represents the Lys/nucleotide unit ratio.

PMPA and PLL was calculated to be 36 and 50, respectively, from the ^{1}H NMR. Diblock copolymers, PEG−PLL with 48 PLL units and PEG−PMPA with 39 PMPA units, were used as comparative samples in this study. The formation of polyplex micelles from these block catiomers was confirmed by a gel retardation assay (Figure S4, Supporting Information).[6] Also, the interaction between the di- or triblock copolymers and plasmid DNA (pDNA) was evaluated by an ethidium bromide (EtBr) exclusion assay (Figure 2a). In the case of PEG−PLL (pK_a 9.4), the fluorescence intensity was decreased to 20% of that of the naked pDNA at the N/P ratio of 2. In contrast, the system of PEG−PMPA, having a cationic segment with a lower pK_a value (pK_a 6.2), maintained relatively high fluorescence (>90%) over a wide range of N/P ratios, suggesting that PEG−PMPA lacks the capacity to condense pDNA to a level detectable by this assay. On the other hand, PEG−PMPA−PLL exhibited an 80% decrease in fluorescence at the N/P ratio of 3. Interestingly, the fluorescence profile of PEG−PMPA−

† Graduate School of Engineering, The University of Tokyo.
‡ Graduate School of Medicine, The University of Tokyo.
§ Nippon Kayaku Co., Ltd.
# CREST, Japan Science and Technology Agency.

10.1021/ja0440506 CCC: $30.25

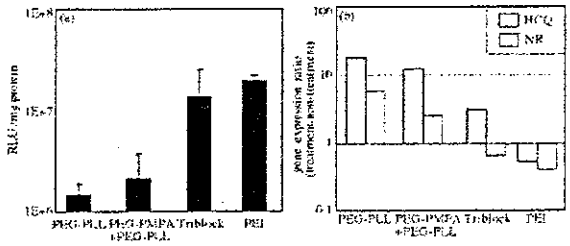

Figure 3. In vitro transfection of luciferase gene to HeLa cells by polyplex micelles from di- or triblock copolymers. HeLa cells were incubated with each micelle in the medium containing 10% serum for 24 h, followed by an additional 24 h incubation without the micelles. (a) The polyplex micelles were prepared at a Lys/nucleotide ratio of 2, and the PEI/pDNA was prepared at the corresponding N/P ratio to the PEG−PMPA−PLL/pDNA. (b) The effects of HCQ and NR on the TE of the polyplexes were evaluated. The PEI polyplex was prepared at the N/P ratio of 10.

PLL/pDNA was almost identical to that of PEG−PLL/pDNA when the N/P ratio was converted to the Lys/nucleotide unit ratio (Figure 2b). Presumably, in the complex of PEG−PMPA−PLL/pDNA, the PLL segment may predominantly contribute to the pDNA condensation. This assumption was confirmed by ^{1}H NMR measurement of PEG−PMPA−PLL/pDNA [Lys/nucleotide ratio = 2 (N/P ratio = 3.4)] in deutereted phosphate-buffered saline (pD 7.4, 150 mM NaCl), in which the chemical shifts assigned to the PLL segment completely disappeared but those assigned to the PMPA segments remained in the spectrum (Figure S6, Supporting Information).[6] This result is consistent with the hypothesis that the PEG−PMPA−PLL/pDNA may form three-layered polyplexes as illustrated in Figure 1. Also, the complete disappearance of PLL peaks from the NMR spectrum suggests that PEG−PMPA−PLL in free form may be minimal in the solution. The size and ζ-potential of the PEG−PMPA−PLL complexes at the Lys/nucleotide ratio of 2 were determined to be 88.7 nm and 7.3 mV, respectively, comparable to those obtained from the PEG−PLL complexes at the N/P ratio of 2 (91.7 nm and 2.1 mV, respectively). The particle size of approximately 100 nm is consistent with the condensed structure of pDNA, and the low absolute value of the ζ-potential suggests the formation of the PEG palisade surrounding the polyplex core.

In vitro transfection efficiency (TE) of the PEG−PMPA−PLL/pDNA at the Lys/nucleotide ratio of 2 was evaluated against HeLa cells. Notably, PEG−PMPA−PLL/pDNA revealed 1 order of magnitude higher TE than PEG-PLL/pDNA (Figure 3a), which was comparable to that of the PEI/pDNA at the corresponding N/P ratio, without showing appreciable cytotoxicity (Figure S9, Supporting Information).[6] On the other hand, the TE of the system composed of (PEG−PMPA + PEG−PLL)/pDNA, where the contents and the repeating units of the PMPA and PLL segments were nearly equal to PEG−PMPA−PLL, was almost the same as that of PEG−PLL. Also, the polyplexes of PEG−PMPA showed no transfection activity over a wide range of N/P ratios (data not shown). These results strongly indicate the importance of aligning in tandem two types of polycations with different pK_a values in a single polymer strand. To study the mechanism of the transfection, the effects of hydroxychloroquine (HCQ) and nigericin (NR) on transfection behavior were investigated. HCQ is known to increase the TE of the polyplexes lacking a buffering capacity, whereas NR could decrease the TE of the polyplexes showing the proton sponge effect.[7] The PEG−PMPA−PLL/pDNA showed less effect of HCQ on enhancing the gene expression compared with the PEG−PLL/pDNA, while it showed an appreciable decrease in the TE in the presence of NR (Figure 3b). Similar trends were also confirmed for 293T cells (Figure S8, Supporting Information). These biological results are consistent with the hypothesis that the enhanced TE of the PEG−PMPA−PLL/pDNA may be attributed to the proton sponge effect. Thus, the buffering capacity of PMPA segment appears to be maintained in the PEG−PMPA−PLL/pDNA under the condition with low Lys/nucleotide ratio. The preferential contribution of the PLL segment to the DNA condensation may ensure the presence of the uncomplexed PMPA segment, even at a comparatively low N/P ratio, to work as a buffering unit.[6]

Nonviral gene vectors used in vivo must have a high stability to be tolerated under harsh conditions in the body. In our previous studies, polyplexes based on PEG−PLL showed a high serum tolerability[8] and prolonged blood circulation.[9] Although the PLL segments form stable polyplexes with pDNA, the transfection activity might be inefficient due to the lack of a proton buffering capacity. In contrast, polycations with a lower pK_a have a buffering capacity for the enhanced transfection but demand a high N/P ratio to achieve a high efficacy. Polyplexes formed at a high N/P ratio may not be useful for in vivo transfection due to stability and toxicity concerns.[5] The result reported here led to the novel design of nonviral gene vectors, overcoming the problems of conventional systems based on the proton sponge concept, using the A−B−C type triblock copolymers, PEG−PMPA−PLL (Figure 1). The results are consistent with the hypothesis that PEG−PMPA−PLL might form three-layered polyplex micelles consisting of a core of pDNA/PLL polyion complexes, an intermediate layer of PMPA segments with a buffer capacity, and an outer shell of biocompatible PEG segments. The PEG−PMPA−PLL polyplexes showed a significantly enhanced transfection activity through the buffering capacity of the PMPA segment, while efficiently compacting pDNA by the PLL segment. Importantly, this increased transfection was achieved under the condition where free or loosely associated polycations are assumed to be minimal, facilitating the future utility of this polyplex micelle for in vivo gene delivery.

Acknowledgment. This work was supported by the Core Research for Evolutional Science and Technology (CREST) from the Japan Science and Technology Agency (JST).

Supporting Information Available: Synthetic method and characterization of triblock copolymers as well as additional data on the physicochemical and biological properties of the PEG−PMPA−PLL/pDNA. This material is available free of charge via the Internet at http://pubs.acs.org.

References

(1) (a) Boussif, O.; Lezoualc'h, F.; Zanta, M. A.; Mergny, M. D.; Scherman, D.; Demeneix, B.; Behr, J.-P. *Proc. Natl. Acad. U.S.A.* **1995**, *92*, 7297−7301. (b) Tang, M. X.; Szoka, F. C. *Gene Ther.* **1997**, *4*, 823−832. (c) Midoux, P.; Monsigny, M. *Bioconjugate Chem.* **1999**, *10*, 406−411. (d) Cherng, J.-Y.; Wetering, P.; Talsma, H.; Crommelin, D. J. A.; Hennink, W. E. *Pharm. Res.* **1996**, *13*, 1038−1042.
(2) Behr, J.-P. *Chemia* **1997**, *51*, 34−36.
(3) Kabanov, A. V.; Bronich, T. K.; Kabanov, V. A.; Yu, K.; Eisenberg, A. *Macromolecules* **1996**, *29*, 6797−6802.
(4) The ratio of the cationic moiety in polycations to the phosphate in DNA.
(5) Boeckle, S.; Gersdorff, K.; Piepen, S.; Culmsee, C.; Wagner, E.; Ogris, M. *J. Gene Med.* **2004**, *6*, 1102−1111.
(6) See Supporting Information.
(7) Lim, Y.-B.; Kim, S.-M.; Suh, H.; Park, J.-S. *Bioconjugate Chem.* **2002**, *13*, 952−957.
(8) (a) Itaka, K.; Harada, A.; Nakamura, K.; Kawaguchi, H.; Kataoka, K. *Biomacromolecules* **2002**, *3*, 841−845. (b) Itaka, K.; Yamauchi, K.; Harada, A.; Nakamura, K.; Kawaguchi, H.; Kataoka, K. *Biomaterials* **2003**, *24*, 4495−4506.
(9) Harada-Shiba, M.; Yamauchi, K.; Harada, A.; Takamisawa, I.; Shimokado, K.; Kataoka, K. *Gene Ther.* **2002**, *9*, 407−414.

JA0440506

Lactosylated Poly(ethylene glycol)-siRNA Conjugate through Acid-Labile β-Thiopropionate Linkage to Construct pH-Sensitive Polyion Complex Micelles Achieving Enhanced Gene Silencing in Hepatoma Cells

Motoi Oishi, Yukio Nagasaki, Keiji Itaka, Nobuhiro Nishiyama, and Kazunori Kataoka

Department of Materials Science and Technology, Tokyo University of Science, 2641 Yamazaki, Noda, Chiba 278-8510, Japan, Department of Orthopaedic Surgery, Faculty of Medicine, The University of Tokyo, 7-3-1 Hongo, Bunkyo-ku, Tokyo 113-8655, Japan, and Department of Materials Science and Engineering, Graduate School of Engineering, The University of Tokyo, 7-3-1 Hongo, Bunkyo-ku, Tokyo 113-8656, Japan

JOURNAL OF THE AMERICAN CHEMICAL SOCIETY®

Reprinted from
Volume 127, Number 6, Pages 1624–1625

J|A|C|S
COMMUNICATIONS

Published on Web 01/22/2005

Lactosylated Poly(ethylene glycol)-siRNA Conjugate through Acid-Labile β-Thiopropionate Linkage to Construct pH-Sensitive Polyion Complex Micelles Achieving Enhanced Gene Silencing in Hepatoma Cells

Motoi Oishi,[†,⊥] Yukio Nagasaki,*[,†,⊥] Keiji Itaka,[‡] Nobuhiro Nishiyama,[§] and Kazunori Kataoka*[,§]

Department of Materials Science and Technology, Tokyo University of Science, 2641 Yamazaki, Noda, Chiba 278-8510, Japan, Department of Orthopaedic Surgery, Faculty of Medicine, The University of Tokyo, 7-3-1 Hongo, Bunkyo-ku, Tokyo 113-8655, Japan, and Department of Materials Science and Engineering, Graduate School of Engineering, The University of Tokyo, 7-3-1 Hongo, Bunkyo-ku, Tokyo 113-8656, Japan

Received August 20, 2004; E-mail: kataoka@bmw.t.u-tokyo.ac.jp; nagasaki@nagalabo.jp

Nucleic acid medicines such as antisense DNAs[1] and small, interfering RNAs (siRNAs)[2] have attracted much attention as a new class of therapeutic agents. In particular, siRNAs are recently recognized as the most powerful tools for sequence-specific gene silencing via naturally occurring RNA interference (RNAi) process.[3] Nevertheless, the therapeutic value of siRNAs under in vivo conditions is still controversial due to their low stability against enzymatic degradation, low permeability across cell membrane, and preferential liver and renal clearance.[4] A major key to the therapeutic success of siRNA is believed to be the development of carrier systems achieving the modulated disposition in the body through the intravenous route as well as the smooth transport of intact siRNA into the interior of the target cell. Worth noticing in this regard is a new class of nanometric-scaled carriers (nanocarriers) of oligonucleotides formulated through the self-assembly of PEG-based block ionomers (polyion complex (PIC) micelles).[5] Both combinations of PEG-*block*-polycation/oligonucleotide and PEG-*block*-oligonucleotide (or PEG-oligonucleotide conjugate)/polycation are feasible for PIC micelle formulation with a segregated PIC core surrounded by a palisade of flexible and hydrophilic PEG layers to increase biocompatibility and enzymatic tolerability. Ligands may be installed on the periphery of the PEG palisade of the PIC micelles to increase the uptake into the target cells through a receptor-mediated endocytotic pathway.[6] A unique finding, which we would like to communicate here, is the remarkably enhanced RNAi in cultured hepatoma cells through the assembly of siRNA into smart lactosylated-PIC micelles with pH-sensitive dissolution properties, thus achieving an appreciable silencing of the target gene at an extremely low siRNA concentration.

Our strategy of formulating pH-sensitive and targetable PIC micelles of siRNA is based on the novel conjugation of siRNA with lactosylated PEG through acid-labile linkage of β-thiopropionate (Lac-PEG-siRNA; Figure 1), followed by the complexation with poly(L-lysine). Note that β-thiopropionate linkage (3-sulfanylpropionyl linkage)[7] is readily cleaved at the pH corresponding to that of the intracellular endosomal compartment (pH = 5.5).[5a] Michael addition of the 5′-thiol-modified sense RNA (firefly luciferase, pGL3-control sense sequence) toward the ω-acrylate group of the α-lactosyl-ω-acryl-PEG gave a conjugate of Lac-PEG with single-stranded RNA (Lac-PEG-ssRNA), which revealed a retarded migration in gel electrophoretic assay (Figure 2, lane 3) compared to free-sense RNA (Figure 2, lane 1) in line with

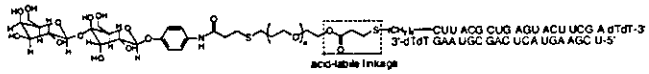

Figure 1. Chemical structure of the Lac-PEG-siRNA conjugate.

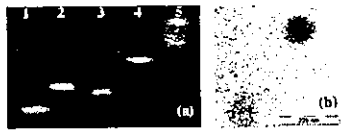

Figure 2. (a) Polyacrylamide gel retardation assay: lane 1, sense RNA; lane 2, siRNA; lane 3, Lac-PEG-ssRNA; lane 4, Lac-PEG-siRNA; and lane 5, PIC micelle. (b) Transmission electron micrograph of the disulfide cross-linked PIC micelle.

PEGylation. Then, the Lac-PEG-ssRNA was annealed with antisense RNA to undergo hybridization, preparing the Lac-PEG conjugate with siRNA (Lac-PEG-siRNA). The Lac-PEG-siRNA thus prepared gave a single band in gel electrophoresis (lane 4) and had further retarded migration compared to Lac-PEG-ssRNA (lane 3) and free siRNA (lane 2). All of these results are consistent with the successful preparation of the Lac-PEG-siRNA with negligible contamination with unreacted and intermediate compounds.

The PIC micelles from the Lac-PEG-siRNA conjugate and PLL (degree of polymerization = 40) were then prepared at the charge ratio of 1 (N/P = 1), where no free Lac-PEG-siRNA conjugate and almost complete retardation were observed in a polyacrylamide gel electrophoresis (Figure 2a, lane 5), suggesting that polyion complexation between the siRNA segment and the PLL quantitatively took place. The PIC micelle with disulfide cross-linked core was also prepared by using thiolated PLL (see Supporting Information) tolerable for the transmission electron microscopy (TEM) observation. As seen in Figure 2b, the disulfide cross-linked PIC micelles have spherical shapes with an average size (n = 36) of 117 ± 26 nm, consistent with the formation of multimolecular micellization of the Lac-PEG-siRNA with PLL.

The dual luciferase reporter assay was done in HuH-7 cells (human hepatoma cells) possessing asialoglycoprotein (ASGP) receptors, which recognize compounds bearing terminal galactose moieties,[8] to evaluate the gene silencing ability of the conjugate and the PIC micelle system (Figure 3). Both the Lac-PEG-siRNA conjugate and the PIC micelle (N/P = 1) revealed RNAi activities with a dose-dependent manner even in the presence of 10% FBS, and in particular, the PIC micelles achieved far more effective RNAi activity than the Lac-PEG-siRNA conjugate alone, viz., 50% inhibitory concentration (IC_{50}) was found to be 1.3 nM and 91.4 nM for the PIC micelle and Lac-PEG-siRNA conjugate, respec-

† Tokyo University of Science.
‡ Faculty of Medicine, The University of Tokyo.
§ Graduate School of Engineering, The University of Tokyo.
⊥ Current address: Tsukuba Research Center for Interdisciplinary Materials Science (TIMS), University of Tsukuba, 1-1-1 Tennoudai, Tsukuba, Ibaragi 305-8573, Japan.

10.1021/ja044941d CCC: $30.25

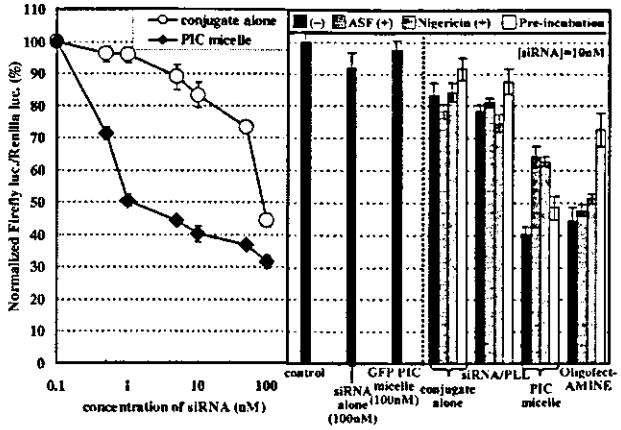

Figure 3. RNAi activities against the firefly luciferase gene generated in cultured HuH-7 cells. Normalized ratios between the firefly luciferase activity (firefly luc.) and the renilla luciferase activity (renilla luc.) are shown on the ordinate. The indicated concentrations of siRNA were the final concentrations in the total transfection volume (250 μL). The plotted data are averages of triplicate experiments ± SD. $P^* < 0.05$ (vs Lac-PEG-siRNA conjugate).

tively. This almost 100 times increase in RNAi activity by PIC micelle is remarkable.

On the other hand, no RNAi activity was observed for free siRNA even at 100 nM of siRNA concentration. The lack of RNAi activity for free siRNA may be ascribed to the low tolerability against enzymatic attack[5a] and/or the restricted uptake into the cellular interior due to the elcetrostatic repulsion with the negatively charged plasma membranes. Note that the PIC micelle including a GFP sequence induced no RNAi, strongly suggesting that an inhibition of firefly luciferase expression observed here indeed occurred through the sequence-specific RNAi effect. In addition, siRNA/PLL (polyplex) showed significantly lower RNAi activity compared to the PIC micelle probably owing to the aggregation at charge-neutralized conditions (N/P = 1) and nonspecific interaction with serum proteins. Although the RNAi activity for the PIC micelle at 10 nM of conjugate concentrations was the same level compared to the commercially available oligofectAMINE (cationic liposome), the RNAi activity for the oligofectAMINE after preincubation with 50% serum for 30 min was significantly reduced (56 → 27% inhibition, $P < 0.05$) due to the nonspecifically interacting nature of the cationic carriers with negatively charged serum proteins. In sharp contrast, the PIC micelle still retained the RNAi activity even after preincubation for 30 min with 50% serum due to the segregation of the siRNA into the PEG environment.[9] To confirm the cellular uptake pathway, asialofetuin (ASF) as the inhibitor for the ASGP receptor-mediated endocytosis[10] was added to the culture medium (4 mg/mL). As a consequence, RNAi activities were reduced significantly for the PIC micelles (60 → 36% inhibition, $P < 0.05$), whereas there was negligible effect of ASF on RNAi activities for Lac-PEG-siRNA conjugate, siRNA/PLL, and oligofectAMINE in HuH-7 cells (Figure 3). Note that no effect of ASF was observed for ASGP receptor-negative NIH 3T3 cells (mouse fibroblast) even for the PIC micelles (see Supporting Information). Obviously, these results indicate that the lactose moieties clustering on the surface of PIC micelle appreciably facilitates ASGP receptor-mediated endocytosis to direct a remarkable RNAi efficacy. Then, nigericin as the inhibitor for the endosomal acidification[11] was added to the culture medium (5 μM) to confirm that the acid-labile linkage in the conjugate contributes RNAi activity. Consequently, the RNAi activity was significantly reduced for the PIC micelle (60 → 37% inhibition, $P < 0.05$), whereas no effect was observed for the Lac-PEG-siRNA conjugate, siRNA/PLL, and the oligofectAMINE. This result suggests that after the endocytotic internalization the cleavage of the acid-labile linkage of the micelles occurred in the manner synchronized with the pH decrease in the endosomal compartment, releasing hundreds of free PEG strands to increase the colloidal osmotic pressure. This may induce the swelling and disruption of the endosome,[12] facilitating the transport of free siRNA into the cytoplasm. Several important factors are likely to be synergistically involved in the pronounced RNAi activity of the PIC micelles, such as the improvement of the stability against enzymatic degradation, minimal interaction with serum proteins, enhancement of the cellular uptake through the ASGP receptor-mediated endocytosis, and the effective transport of free siRNA from endosome into cytoplasm. It should be noted that the PIC micelles entrapping the Lac-PEG-siRNA conjugate reported here showed about 5800 times higher gene-silencing effect compared to that entrapping the Lac-PEG-antisense DNA conjugate targeting the same gene sequence (IC_{50} = 7.6 μM).[13]

In conclusion, the pH-responsive and targetable PIC micelle composed of PLL and Lac-PEG-siRNA conjugate bearing an acid-labile linkage exhibited significant gene silencing for firefly luciferase expression in HuH-7 cells. Therefore, this approach of PIC micellization of PEG-siRNA conjugate with an appropriate polycation has promise as a targetable siRNA delivery system used in a practical context. Further study on gene silencing against endogenous genes as well as in vivo performance is now in progress in our laboratories.

Acknowledgment. This work was supported by the Core Research for Evolutional Science and Technology (CREST) from the Japan Science and Technology Agency [JST]. We appreciate Mr. Teisaku Nakamura for taking the TEM image.

Supporting Information Available: Experimental details, materials, and the dual luciferase reporter assay. This material is available free of charge via the Internet at http://pubs.acs.org.

References

(1) (a) Crooke, S. T. *Biotechnol. Genet. Eng. Rev.* **1998**, *15*, 121. (b) Cook, P. D. *Handb. Exp. Pharmacol.* **1998**, *131*, 51.
(2) Elbashir, S. M.; Harborth, J.; Lendeckel, W.; Yalcin, A.; Weber, K.; Tuschl, T. *Nature* **2001**, *411*, 494.
(3) Taira, H. K. *Nucleic Acid Res.* **2003**, *31*, 700. (c) Miyagishi, M.; Taira, K. *Nat. Biotechnol.* **2002**, *20*, 497.
(4) Braasch, D.; Paroo, Z.; Constantiescu, A.; Ren, G.; Öz, O. K.; Mason, R. P.; Corey, D. R. *Bioorg. Med. Chem. Lett.* **2004**, *14*, 1139.
(5) For selected examples, see: (a) Oishi, M.; Sasaki, S.; Nagasaki, Y.; Kataoka, K. *Biomacromolecules* **2003**, *4*, 1426. (b) Jeong, J. H.; Kim, S. W.; Park, T. G. *Bioconjugate Chem.* **2003**, *14*, 473. (c) Vinogradov, S. V.; Bronich, T. K.; Kabanov, A. V. *Bioconjugate Chem.* **1998**, *9*, 805. (d) Kataoka, K.; Togawa, H.; Harada, A.; Yasugi, K.; Matsumoto, T.; Katayose, S. *Macromolecules* **1996**, *29*, 8556. (e) Harada, A.; Kataoka, K. *Macromolecules* **1995**, *28*, 5294.
(6) Wakebayashi, D.; Nishiyama, N.; Yamasaki, Y.; Itaka, K.; Kanayama, N.; Harada, A.; Nagasaki, Y.; Kataoka, K. *J. Controlled Release* **2004**, *95*, 653.
(7) Schoenmakers, R. G.; van de Wetering, P.; Elbert, D. L.; Hubbell, J. A. *J. Controlled Release* **2004**, *95*, 291.
(8) Wu, C. H.; Wu, G. Y. *Adv. Drug Delivery Rev.* **1998**, *29*, 243.
(9) Itaka, K.; Kanayama, N.; Nishiyama, N.; Jang, W.-D.; Yamasaki, Y.; Nakamura, K.; Kawaguchi, H.; Kataoka, K. *J. Am. Chem. Soc.* **2004**, *126*, 13612.
(10) Zanta, M. A.; Boussif, O.; Adib, A.; Behr, J. P. *Bioconjugate Chem.* **1997**, *8*, 839.
(11) Uherek, C.; Fominaya, J.; Wels, W. *J. Biol. Chem.* **1998**, *273*, 8835.
(12) Goh, S. L.; Murthy, N.; Xu, M.; Fréchet, J. M. J. *Bioconjugate Chem.* **2004**, *15*, 467.
(13) Oishi, M.; Nagatsugi, F.; Sasaki, S.; Nagasaki, Y.; Kataoka, K. *ChemBioChem.* In press.

JA044941D

Drug Delivery

Supramolecular Nanocarrier of Anionic Dendrimer Porphyrins with Cationic Block Copolymers Modified with Polyethylene Glycol to Enhance Intracellular Photodynamic Efficacy**

*Woo-Dong Jang, Nobuhiro Nishiyama, Guo-Dong Zhang, Atsushi Harada, Dong-Lin Jiang, Satoko Kawauchi, Yuji Morimoto, Makoto Kikuchi, Hiroyuki Koyama, Takuzo Aida, and Kazunori Kataoka**

A great number of challenges have been overcome to create efficient photosensitizers (PSs) for photodynamic therapy (PDT) which have a high photocytotoxicity and selectivity for

[*] Dr. W.-D. Jang, Dr. N. Nishiyama, Dr. G.-D. Zhang, Dr. A. Harada, Prof. Dr. K. Kataoka
Department of Materials Science and Engineering
Graduate School of Engineering, The University of Tokyo
7-3-1 Hongo, Bunkyo-ku, Tokyo 113-8656 (Japan)
Fax: (+81) 3-5841-7139
E-mail: kataoka@bmw.t.u-tokyo.ac.jp

Dr. D.-L. Jiang, Prof. Dr. T. Aida
Department of Chemistry and Biotechnology
Graduate School of Engineering, The University of Tokyo
7-3-1 Hongo, Bunkyo-ku, Tokyo 113-8656 (Japan)

Dr. W.-D. Jang, Dr. G.-D. Zhang, Dr. A. Harada, Prof. Dr. K. Kataoka
CREST
Japan Science and Technology Corporation (Japan)

Dr. N. Nishiyama, Dr. H. Koyama
Department of Clinical Vascular Regeneration
Graduate School of Medicine, The University of Tokyo
7-3-1 Hongo, Bunkyo-ku, Tokyo 113-8655 (Japan)

Dr. S. Kawauchi, Dr. Y. Morimoto, Prof. Dr. M. Kikuchi
Department of Medical Engineering
National Defense Medical College
3-2 Namiki, Tokorozawa, Saitama, 359-8513 (Japan)

[**] This work was supported by Core Research for Evolutional Science and Technology (CREST), JST.

 DOI: 10.1002/anie.200461603

the diseased tissue.[1] To obtain high quantum yields and effective energy absorption, PSs generally need to have large π-conjugation domains such as a porphyrin structure. Therefore, most conventional PSs easily form aggregates, which produce a self-quenching effect of the excited state, in aqueous medium as a result of their π–π interactions and hydrophobic characteristics. These issues can be overcome, as we reported previously, by segregating PSs into the focal core of dendrimers (dendrimer porphyrins (DPs), Figure 1b).[2] DPs are attractive for biomedical purposes because of their predictable structures, that is, their monodisperse molecular weight and tunable three-dimensional structures, and their flexibility for a high density of tailored functional groups on the periphery.[3] Indeed, third-generation DPs with 32 cationic or anionic peripheral groups exhibit a high solubility in aqueous medium and have a high quantum yield for the generation of singlet oxygen, which leads to an appreciable photocytotoxicity.[2] These advantageous features of DPs are facilitated to an even greater extent by their inclusion into stealth nanocarriers, thus improving their longevity in blood circulation and results in their gradual accumulation in solid tumors through the enhanced permeation and retention (EPR) effect.[4] Furthermore, as demonstrated here, the inclusion of DPs into a novel type of nanocarrier, that is, polymeric micelles, has led to an unprecedented increase in the photocytotoxicity without compromising either the photophysical properties of DPs in regard to their efficient photochemical reactions or the physicochemical properties of the carriers necessary for tumor-selective delivery.

A novel polymeric micelle system[5] for PDT is based on an electrostatic assembly of an anionic DP,[6] which consists of zinc porphyrin at the focal core with a third generation of poly(benzyl ether) dendritic frameworks having 32 negative charges on the periphery, and poly(ethylene glycol)–poly(L-lysine) block copolymer (PEG-*b*-PLL) in aqueous media (polyion complex (PIC) micelles; Figure 1b).[7] The DP-incorporated micelles (DP/m), prepared with a stoichiometric ratio of negatively charged DP and positively charged PEG-*b*-PLL, were approximately 64 nm in diameter with an extremely narrow size distribution in physiological saline solution (Figure 2a). Our previous study using static light scattering (SLS) measurements demonstrated that an individual DP/m contains an average of 38 DP molecules and the micelles have a remarkable stability against salt concentrations,[7] which indicates the clear stabilization effect by the 32 negative charges of DP in the micellar structure. The dependency of the formation of DP/m on the pH value was investigated by dynamic and static light scattering (DLS and SLS) measurements. Figure 2b shows the pH-dependent changes in the translational diffusion coefficient (D_T) and normalized $(Kc/\Delta R(0))^{-1}$ (normalized to the micelle at pH 7.4) of DP/m, where D_T is related to the hydrodynamic size based on the Stokes–Einstein equation, and the normalized $(Kc/\Delta R(0))^{-1}$ value is related to the changes in the average apparent molecular weight of the micelles. Both the hydrodynamic size and normalized $(Kc/\Delta R(0))^{-1}$ value basically remained unchanged in the pH range from 6.4 to 8.5 (Figure 2b). However, the diameter of the micelles gradually

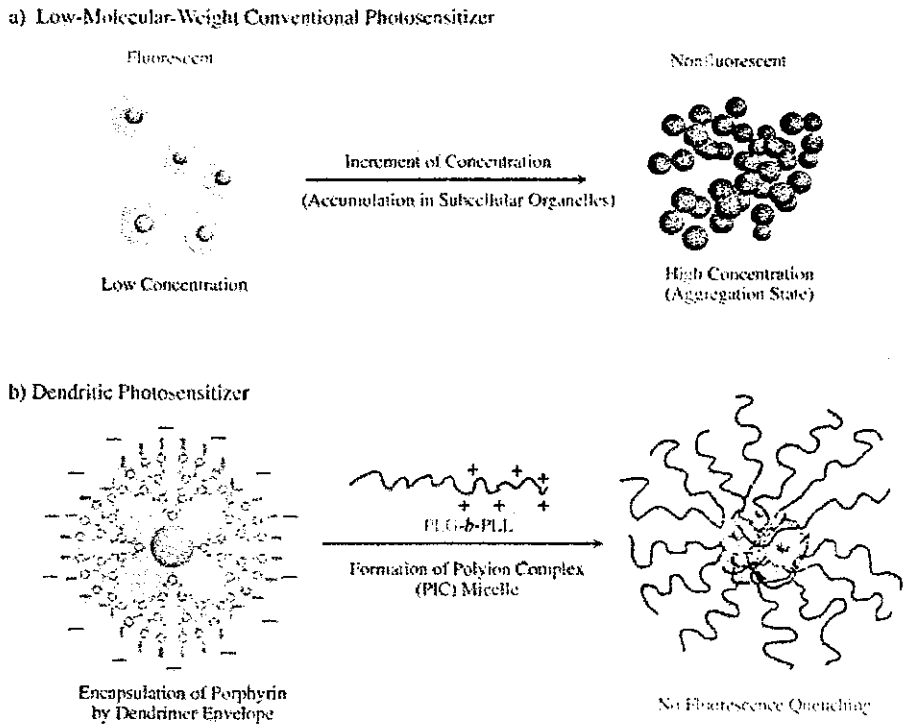

Figure 1. a) Conventional PS aggregate at a high concentration which results in quenching of PSs. b) Formation of polyion complex (PIC) micelles through electrostatic assembly of anionic dendrimer porphyrins (DPs) and PEG-*b*-PLL copolymers. The dendrimer envelope of DP can sterically prevent aggregation of the center porphyrin, thus there is no fluorescence quenching of the center porphyrin.

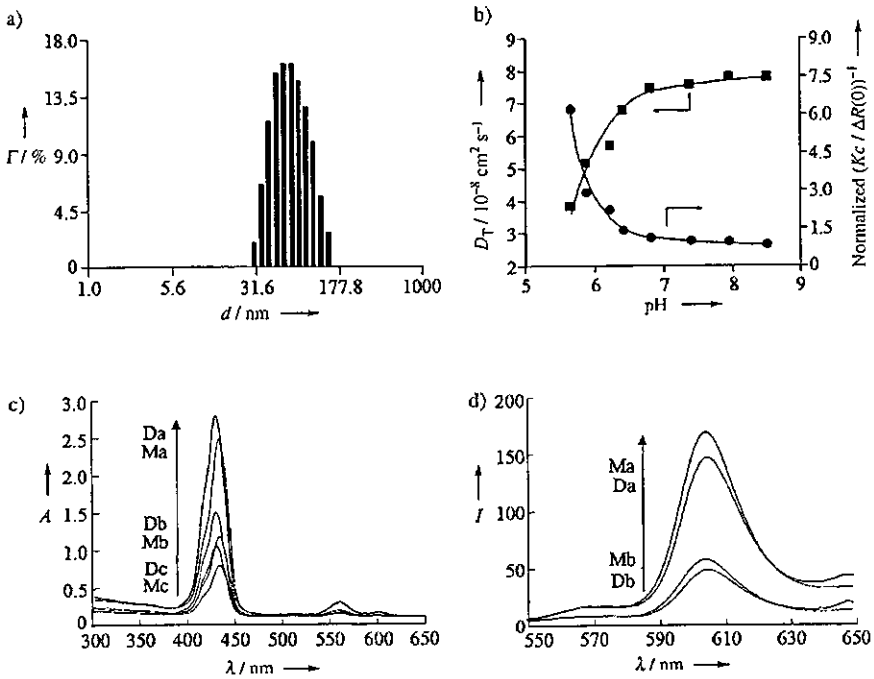

Figure 2. Physical properties of DP and DP/m. a) DLS histogram of DP/m in 150 mM NaCl at 25 °C; d = diameter. b) Dependency of the translational diffusion coefficients D_T (■) and normalized $(Kc/\Delta R(0))^{-1}$ (●) on the pH value for DP/m (1 mg mL^{-1}), measured by DLS and SLS, respectively, at 25 °C. c) Electronic absorption spectra of DP alone and DP/m in PBS (pH 7.4; a = 12 μM, b = 4 μM, c = 2 μM, D: DP, M: DP/m). d) Fluorescence emission spectra of DP alone and DP/m in PBS (pH 7.4; a = 12 μM, b = 4 μM, D: DP, M: DP/m).

increased with an increased apparent molecular weight below pH 6.4 (Figure 2b), and finally precipitated at pH 5.6, which indicates the acid-responsive feature of the micelles. Protonation of DP occurred under acidic pH conditions and resulted in the diminution of the electrostatic interaction between DP and PEG-*b*-PLL. Thus, the well-defined core–shell structure may become more diffuse and a merging of the micelles may take place. This pH-responsive behavior of the micelles allows their effective accumulation in solid tumors in response to the low pH value of the tumor tissue[8] or in an endosomal compartment in the tumor cells while achieving stable circulation in the bloodstream.

The electronic absorption and emission spectra of DP and DP/m are shown in Figure 2c and d, respectively. Unlike low-molecular-weight PSs,[9] DP clearly maintained its absorption and emission intensity in spite of the formation of micelles. The incorporation of DP into the micelles resulted in a 5-nm red-shift for the Soret band of the porphyrin core and a hypochromicity of about 5% (Figure 2c). Both of these effects are likely to be caused by the formation of an electrostatic assembly of charged porphyrins and oppositely charged compounds.[10] The shrinkage of the hydrophobic dendrimer frameworks, which arises from the relaxation of the charge repulsion of the negatively charged DP surface by the formation of an electrostatic assembly, may contribute to the hypochromicity.[11] Interestingly, although the local concentration of DP within each micelle is assumed to be extremely high, DP/m emitted a more intense fluorescence at 610 nm (Figure 2d). Unlike conventional PSs, the dendritic envelope of DP is able to prevent the porphyrin core from undergoing collisional quenching, even at an appreciably high concentration that induces self-quenching of the conventional PSs (Figure 1a).[12] Thus, encapsulation of the porphyrins by the dendritic envelope in the micellar structure is most likely to prevent fluorescence quenching (Figures 1b and 2d). Also, the high microviscosity in the micellar core could restrain the internal molecular motion of DP, which might lead to the inhibition of the nonradiative decay and is related to the increased fluorescence intensity of DP/m (Figure 2d).[13] In connection with this observation, the photoinduced oxygen consumption of DP and DP/m was measured in phosphate-buffered saline (PBS) containing 10% fetal bovine serum (FBS) as a singlet oxygen acceptor (Figure 3). Very interestingly, the result revealed that the oxygen consumption level of

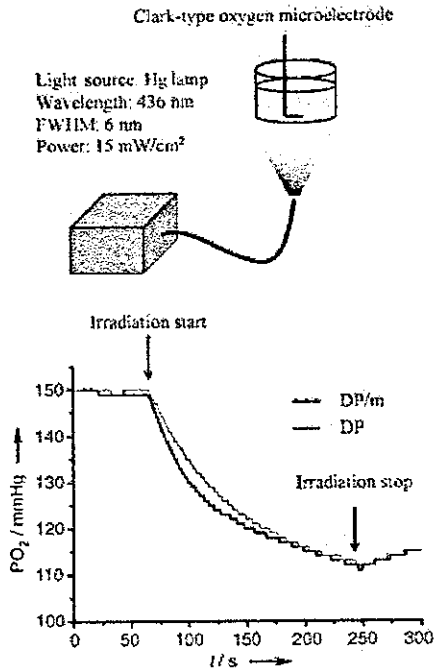

Figure 3. Experimental setup for the measurement of oxygen consumption and the results obtained. FWHM = full width of half maximum height.

DP/m was almost identical to that of the free DP in PBS, which indicates that the singlet oxygen molecules can successfully escape the micellar structure. From the standpoint of the application to PDT, the DP ensures an effective photochemical reaction of the porphyrin core regardless of the local concentrations. It is possible that the DP/m attain an elevated concentration of local singlet oxygen, which cannot be achieved by other formulations containing conventional PSs.

However, the cellular uptake of free DP and DP/m increased with the incubation time, and DP/m showed six- to eightfold higher uptake levels than free DP (Figure 4a). In

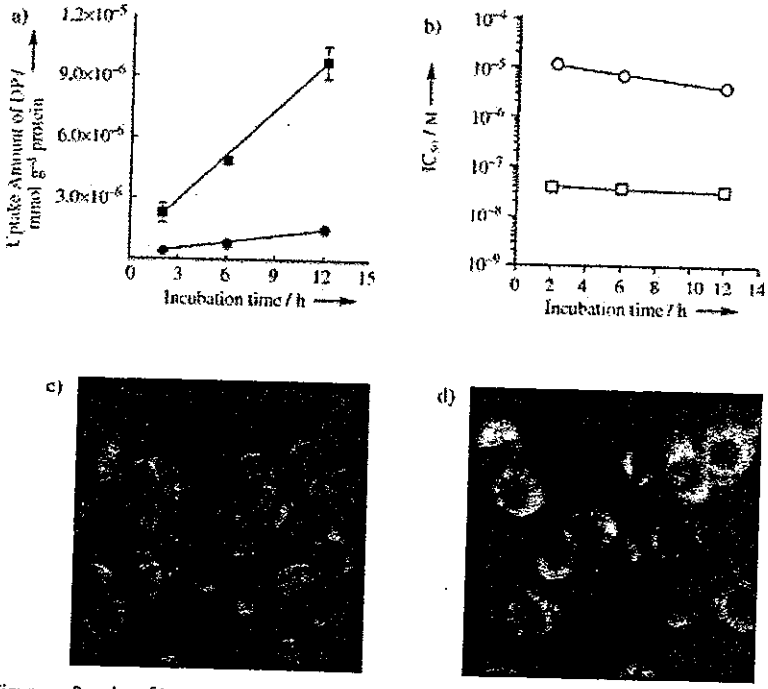

Figure 4. Results of in vitro evaluations of DP and DP/m. a) Cellular uptake level of DP (●) and DP/m (■) as a function of incubation time ($n=3$). LLC cells were incubated with dendrimers and the micelles at 12 μM of DP-equivalent concentration. b) Incubation time dependency of 50% growth inhibitory concentration (IC_{50}) of DP (○) and DP/m (□) after photoirradiation. c, d) Microscopy images of LLC cells incubated with 10 μM of DP (c) and DP/m (d) for 8 h. A Zeiss filter set (excitation: BP 395–440 nm; beam splitter: FT 460 nm; emission: LP 470 nm) was used.

view of the negatively charged surface of mammalian cells,[8] charge neutralization of DP by PEG-*b*-PLL could improve the cellular uptake of DP/m. The improved uptake of DP/m was also confirmed by microscopic observations (Figure 4c and d). No fluorescence quenching was observed for the cells incubated with DP/m, although the sensitizers are assumed to be extremely concentrated in the subcellular organelles such as the endosomes and lysosomes. This observation contrasts with the fact that the conventional mesochlorin e_6 conjugated *N*-(2-hydroxypropyl) methacrylamide (HPMA) copolymers exhibit fluorescence quenching when the cells are incubated with HPMA at an extremely high concentration.[14] The dendritic envelope of DP could prevent aggregation of the porphyrin in the subcellular loci, thus ensuring effective production of singlet oxygen for the photocytotoxicity.

Notably, the photocytotoxicity of DP/m was remarkably improved compared to that of free DP (Figure 4b). Incorporation of DP into the micelles resulted in an approximately 130–280-fold increased photocytotoxicity (Figure 4b). Such a distinctly enhanced photocytotoxicity of DP/m may not be fully explained by the six- to eightfold increase in their cellular uptake shown in Figure 4a; therefore, DP/m may have specific mechanisms to increase their photocytotoxicity. Recently, PEGylated chlorin e_6 and PEG-based polymeric micelles were reported to show an enhanced localization in several cytoplasmic organelles including the mitochondria.[15] Presumably the outer PEG layer of the DP/m and the microenvironment around DP, as mentioned above, may have a role in altering the intracellular mechanism of DP to increase the photocytotoxicity. Recently, several interesting observations concerning the intracellular mechanism have been reported. For example, Berg et al. proposed a photochemical internalization (PCI) in which the photodamage to endosomal membranes can burst the endocytic vesicles, which allows endosomal escape of macromolecules into the cytosol.[16] From this point of view, DP/m may localize in the cytoplasmic organelles susceptible to photodamage following endosomal escape of the micelles during photoirradiation. The DP/m are assumed to produce a significantly high concentration of singlet oxygen as a result of effective separation of the center porphyrin by the dendritic envelope. The mechanism for the efficient generation of singlet oxygen within the micellar structure remains to be explained. However, a dendritic structure that prevents aggregation of the center porphyrin should be essential for the enhanced photocytotoxicity of DP/m. Further investigation to address the detailed mechanisms of the enhanced photocytotoxicity of DP/m, together with dendrimer size and morphological effect, is now in progress.

In summary, the photodynamic efficacy of the DP was dramatically improved by inclusion into micelles. This process resulted in a more than two orders of magnitude increase in the photocytotoxicity compared with that of the free DP, as a result of the accumulated singlet oxygen in the intracellular compartment as well as the modulated intracellular localization related to the micellar structure. Furthermore, the DP/m system has a relevant size range (ca. 100 nm) and high stability for intravenous administration, with resultant EPR effect, and may have a high utility for in vivo PDT of cancer and macular degeneration, the study of which is now in progress.

Experimental Section

PEG-*b*-PLL was synthesized by the polymerization of the *N*-carboxy anhydride of N^{ε}-Z-L-lysine initiated by CH_3O-PEG-NH_2 (12000 g mol^{-1}) in DMF, followed by deprotection of the Z group according to a previously reported method.[17] The M_w/M_n ratio and degree of polymerization of PLL were determined to be 1.11:1 and 41 by gel-permeation chromatography and ^{1}H NMR spectroscopy,

respectively. DP was synthesized as previously described,[6] and its purity was confirmed by a single peak in the MALDI-TOF mass spectrum (8030 g mol^{-1}). The DLS and SLS measurements of DP/m were performed using a Photal dynamic laser-scattering DLS-7000 spectrometer (Otsuka Electronics Co., Ltd., Osaka, Japan). The UV/Vis and fluorescence spectra were measured on a V-550 spectrophotometer and on an FP-777 spectrofluorometer (JASCO, Tokyo, Japan), respectively.

Lewis lung carcinoma (LLC) cells were used in the cell culture studies. In the quantitative analysis of the cellular uptake of DP, the cells incubated with free DP and DP/m were lyzed in 5% SDS solution, followed by measurement of the fluorescence intensity at 609 nm (excitation at 432 nm). In the cytotoxicity assay, the cells were photoirradiated for 10 minutes with broadband visible light using a xenon lamp (150 W) equipped with a filter passing light of 400–700 nm (fluence energy: 180 kJ cm^{-2}). The viability of the cells was evaluated by the 3-(4,5-dimethylthiazol-2-yl)-2,5-diphenyltetrazolium bromide (MTT) assay.

Oxygen consumption was measured by using a Clark-type oxygen microelectrode with a tip diameter of 200 μm (PO_2-100DW, Eikou Kagaku Co., Ltd., Tokyo, Japan). The microelectrode was inserted into the PBS, which contained 3.13 μM of DP or DP/m and 10% FBS as a singlet oxygen acceptor, so that the tip was 100 mm above the bottom of the solution. An Hg lamp (436 nm, FWHM: 6 nm, 15 mW cm^{-2}) was used for light irradiation. The solution was static and exposed to the atmosphere. Before each measurement, the system was calibrated in saline solution bubbled with air, in which the oxygen partial pressure was assumed to be 150 mm Hg.

Received: August 10, 2004

Keywords: block copolymers · dendrimers · drug delivery · micelles · porphyrinoids

[1] R. K. Pandey, G. Zhang in *Porphyrin Handbook, Vol. 6* (Eds.: K. M. Kadish, K. M. Smith, R. Guilard), Academic Press, **2000**, pp. 157–230.
[2] N. Nishiyama, H. R. Stapert, G. D. Zhang, D. Takasu, D. L. Jiang, T. Nagano, T. Aida, K. Kataoka, *Bioconjugate Chem.* **2003**, *14*, 58–66.
[3] a) A. W. Bosman, H. M. Jassen, E. W. Meijer, *Chem. Rev.* **1999**, *99*, 1665–1688; b) S. Hecht, J. M. J. Frechet, *Angew. Chem.* **2001**, *113*, 76–94; *Angew. Chem. Int. Ed.* **2001**, *40*, 74–91; c) M. Fischer, F. Vogtle, *Angew. Chem.* **1999**, *111*, 934–955; *Angew. Chem. Int. Ed.* **1999**, *38*, 884–905; d) H. R. Ihre, L. Gagne, J. M. J. Frechet, F. C. Szoka, Jr., *Bioconjugate Chem.* **2002**, *13*, 453–461; e) J. F. Kukowska-Latallo, A. U. Bielinska, J. Johnson, R. Spindler, D. A. Tomalia, J. R. Baker, *Proc. Natl. Acad. Sci. USA* **1996**, *93*, 4897–4902.
[4] a) Y. N. Konan, R. Gurny, E. Allemann, *J. Photochem. Photobiol. B* **2002**, *66*, 89–106; b) Y. Matsumura, H. Maeda, *Cancer Res.* **1986**, *46*, 6387–6392; c) M. Yokoyama, T. Okano, Y. Sakurai, S. Fukushima, K. Okamoto, K. Kataoka, *J. Drug Targeting* **1999**, *7*, 171–186.
[5] Y. Kakizawa, K. Kataoka, *Adv. Drug Delivery Rev.* **2002**, *54*, 203–222, and references therein.
[6] a) N. Tomioka, D. Takasu, T. Takahashi, T. Aida, *Angew. Chem.* **1998**, *110*, 1611–1614; *Angew. Chem. Int. Ed.* **1998**, *37*, 1531–1534; b) T. Aida, D.-L. Jiang in *The Porphyrin Handbook, Vol. 3* (Eds: K. M. Kadish, K. M. Smith, R. Guilard), Academic Press, **2003**, pp. 369–384.
[7] H. R. Stapert, N. Nishiyama, D. L. Jiang, T. Aida, K. Kataoka, *Langmuir* **2000**, *16*, 8182–8188.
[8] a) E. J. Ambros, D. M. Easty, P. C. T. Jones, *Br. J. Cancer* **1958**, *12*, 439–447; b) S. E. Kornguth, T. Kalinke, H. I. Robins, J. D. Cohen, P. Turski, *Cancer Res.* **1989**, *49*, 6390–6395.
[9] S. A. Gerhardt, J. W. Lewis, D. S. Kliger, J. Z. Zhang, U. Simonis, *J. Phys. Chem. A* **2003**, *107*, 2763–2767.
[10] a) N. C. Maiti, S. Mazumdar, N. Periasamy, *J. Phys. Chem. B* **1998**, *102*, 1528–1538; b) K. M. Kadish, G. B. Maiya, C. Araullo, R. Guilard, *Inorg. Chem.* **1989**, *28*, 2725–2731.
[11] R. Sadamoto, N. Tomioka, T. Aida, *J. Am. Chem. Soc.* **1996**, *118*, 3978–3979.
[12] T. Sato, D.-L. Jiang, T. Aida, *J. Am. Chem. Soc.* **1999**, *121*, 10658–10659.
[13] S. Basu, *J. Photochem. Photobiol. A: Chem.* **1991**, *56*, 339–347.
[14] N. Nishiyama, A. Nori, A. Malugin, Y. Kasuya, P. Kopeckova, J. Kopecek, *Cancer Res.* **2003**, *63*, 7876–7882.
[15] a) M. R. Hamblin, J. L. Miller, T. Hasan, *Cancer Res.* **2001**, *61*, 7155–7162; b) R. Savic, L. Luo, A. Eisenberg, D. Maysinger, *Science* **2003**, *300*, 615–618.
[16] a) K. Berg, P. K. Selbo, L. Prasmickaite, T. E. Tjelle, K. Sandvig, J. Moan, G. Gaudernack, O. Fodstad, S. Kjolsrud, H. Anholt, G. H. Rodal, S. K. Rodal, A. Hogset, *Cancer Res.* **1999**, *59*, 1180–1183; b) L. Prasmickaite, A. Høgset, P. K. Selbo, B. Ø. Engesæter, M. Hellum, K. Berg, *Br. J. Cancer* **2002**, *86*, 652–657.
[17] A. Harada, K. Kataoka, *Macromolecules* **1995**, *28*, 5294–5299.

Supramolecular Nanocarrier of siRNA from PEG-Based Block Catiomer Carrying Diamine Side Chain with Distinctive pK_a Directed To Enhance Intracellular Gene Silencing

Keiji Itaka, Naoki Kanayama, Nobuhiro Nishiyama, Woo-Dong Jang, Yuichi Yamasaki, Kozo Nakamura, Hiroshi Kawaguchi, and Kazunori Kataoka

Department of Materials Science and Engineering, Graduate School of Engineering, and Department of Orthopaedic Surgery, Faculty of Medicine, University of Tokyo, 7-3-1 Hongo, Bunkyo-ku, Tokyo 113-8656, Japan

JOURNAL OF THE AMERICAN CHEMICAL SOCIETY®

Reprinted from
Volume 126, Number 42, Pages 13612–13613

J|A|C|S
COMMUNICATIONS

Published on Web 09/30/2004

Supramolecular Nanocarrier of siRNA from PEG-Based Block Catiomer Carrying Diamine Side Chain with Distinctive pK_a Directed To Enhance Intracellular Gene Silencing

Keiji Itaka,[†,‡] Naoki Kanayama,[†] Nobuhiro Nishiyama,[†] Woo-Dong Jang,[†] Yuichi Yamasaki,[†] Kozo Nakamura,[‡] Hiroshi Kawaguchi,[‡] and Kazunori Kataoka*[,†]

Department of Materials Science and Engineering, Graduate School of Engineering, and Department of Orthopaedic Surgery, Faculty of Medicine, University of Tokyo, 7-3-1 Hongo, Bunkyo-ku, Tokyo 113-8656, Japan

Received May 14, 2004; E-mail: kataoka@bmw.t.u-tokyo.ac.jp

The short double-stranded RNA species, called short interference RNA (siRNA), can be used to silence the gene expression in a sequence-specific manner in a process that is known as RNA interference (RNAi).[1] It has become a useful method for the analysis of gene functions and holds the significant possibility of therapeutic application. However, to promote an efficient gene knockdown, especially in an in vivo situation, two substantial issues must be considered: tolerability under physiological conditions and enhanced cellular uptake. Thus, the development of effective siRNA delivery systems is required.

Recently, a new delivery system of plasmid DNA and oligonucleotides has been developed, based on the micellar assembly of the poly-ion complex (PIC) of these compounds with block copolymers consisting of poly(ethylene glycol) (PEG) and polycation segments, leading to the self-assembled structure with a core−shell architecture (PIC micelles).[2] Their excellent properties for in vivo DNA delivery have been confirmed so far:[3] a diameter around 100 nm with a PEG palisade which enables complexes to avoid recognition by reticuloendothelial systems, increased nuclease resistance, increased tolerance under physiological conditions, and the excellent gene expression in a serum-containing medium.[4]

We now describe the structural design of a novel block catiomer-based PIC particularly available for siRNA delivery. PEG−poly(3-[(3-aminopropyl)amino]propylaspartamide (PEG-DPT; PEG, 12 000 g/mol, polymerization degree of DPT segment, 68), carrying a diamine side chain with distinctive pK_a, was newly synthesized by a side-chain aminolysis reaction of PEG−poly(β-benzyl-L-aspartate) block copolymer (PEG-PBLA) with dipropylene triamine (DPT) (Figure 1A and Figure S1 in the Supporting Information). A model compound of a DPT unit, *tert*-butoxycarbonyl-β-*N*-3-(3-aminopropyl)aminopropylamido-α-*N*-propyl-(L)-aspartamide (Boc-Asp(DPT)-Pr), was also synthesized (see Supporting Information) to determine the pK_a values of the amino groups.

Boc-Asp(DPT)-Pr clearly gave a two-stage pH−α curve (Figure 1B), from which the pK_a values of the primary and secondary amino groups were determined to be 9.9 and 6.4, respectively. Amino groups in the PIC of polyamine with polynucleotides including siRNA generally undergo facilitated protonation due to the zipper effect or the neighboring group effect during the complexation process, hampering the proton buffering or the proton sponge capacity. The unique feature of PEG-DPT is the regulated location of primary and secondary amino groups in the side chain: the former, with higher pK_a, settles at the distal end of the side chain to participate in the ion complex formation with phosphate groups in siRNA molecule, whereas the latter, with lower pK_a, located closer to the polymer backbone, is expected to leave a substantial

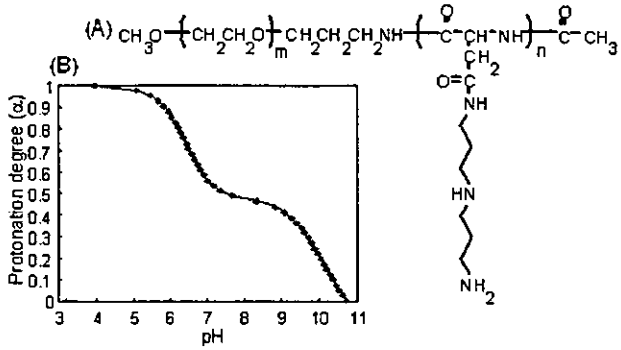

Figure 1. (A) Chemical structure of PEG-DPT. (B) Change in protonation degree (α) with pH for Boc-Asp(DPT)-Pr.

fraction of unprotonated form even in the complex, presumably due to the lower protonation power and the spatial restriction, directing to the enhanced intracellular activity of siRNA through the buffering capacity in the endosomal compartment.

The formation of the siRNA complex with the PEG-DPT was confirmed by polyacrylamide gel electrophoresis (PAGE) and the ethidium bromide (EtBr) exclusion assay (see Figure S2 in the Supporting Information). Note that intercalators such as EtBr bind the double-stranded (ds) RNA in the same fashion as dsDNA.[5] The free siRNA disappeared at the N/P ratio (= [total amines in cationic segment]/[siRNA phosphates]) >2, in line with a substantial fluorescence quenching of EtBr at N/P ≥ 2 due to the inaccessibility of EtBr to the complexed siRNA with PEG-DPT. Furthermore, the EtBr assay highlights the distinctive role of primary and secondary amino groups of the side chain in the complex. The PIC of the double-stranded oligo DNA, composed of sequences similar to the GL3 targeting siRNA, with PEG−poly(3-dimethylamino)propyl aspartamide (PEG-DMAPA; p$K_a \approx 7.9$, see Figure S3 for chemical structure), revealed a lower degree of EtBr quenching compared to the PEG-DPT/ds-oligo DNA PIC, even in the region of excess N/P ratios (see Figure S4), suggesting that the presence of unprotonated amino groups in the former may hamper the tight association. PEG−poly(L-lysine) (PEG-PLL; p$K_a \approx 9.37$, see Figure S3 for chemical structure) induced EtBr quenching as significantly as PEG-DPT upon complexation with the ds-oligo DNA, yet the quenching leveled off at the stoichiometric N/P ratio (N/P = 1.0) (Figure S4). This is in sharp contrast with the PEG-DPT/ds-oligo DNA complex, which showed leveling-off behavior of EtBr quenching at N/P ≈ 2.0, suggesting that secondary amines with the lower pK_a may be excluded from the ion complexation with oligonucleotides.

These distinctive features of the PEG-DPT, PEG-DMAPA, and PEG-PLL complexes indeed correlated with their gene knockdown abilities. For this evaluation, the GL3 luciferase gene was targeted

† Department of Materials Science and Engineering.
‡ Department of Orthopaedic Surgery.

10.1021/ja047174r CCC: $27.50

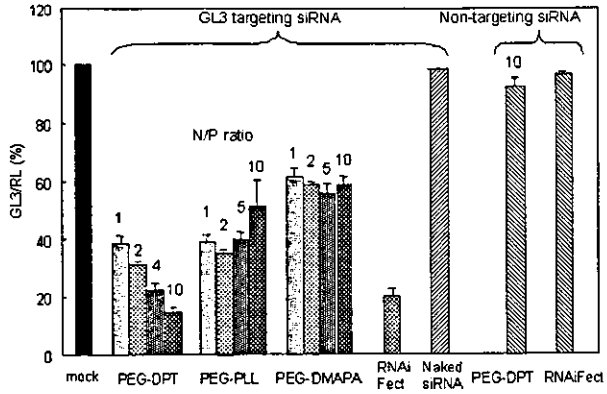

Figure 2. GL3 luciferase gene knockdown (n = 4; ±SD).

after transfecting two kinds of luciferase pDNAs (pGL3 and pRL; Promega) to HuH-7 cells. The expression ratio of GL3/RL was used as the knockdown marker.

Each complex system showed a sufficient knockdown of the GL3 luciferase, while neither the naked siRNA nor the nontargeting siRNA showed any knockdown (Figure 2). Thus, these results should be recognized as the veritable RNAi by the GL3-targeting siRNA delivered into the cytoplasm. Notably, the gene knockdown abilities of the siRNA/PEG-DPT complex were superior to those of the other two complexes, especially at higher N/P ratios. At N/P = 10, it showed more than an 80% knockdown, which exceeded the commercial RNAiFect. The cell viability evaluated by MTT assay was more than 75% of the mock cells, even after co-incubation with siRNA/PEG-DPT with N/P ≥ 10 (see Figure S5), suggesting the toxic effect to be eliminated. The siRNA/PEG-DMAPA complexes showed knockdown abilities to a lesser extent. Apparently, the loosely associated nature of siRNA, suggested by the EtBr exclusion assay, is unfavorable for facilitating an effective intracellular delivery of intact siRNA. PEG-PLL showed a considerable knockdown ability in the low N/P region, yet no particular enhancement with the increase in the N/P ratios. High efficacy of PEG-DPT may be characterized by the existence of additional secondary amines with a lower pK_a to promote the internalization of the siRNA molecules into the cytoplasm through buffering of the endosomal cavity, as is the case with the polyethylenimine-based polyplex that shows an enhanced tranfection efficiency at the higher N/P ratios.[6]

A serum incubation study was then performed to evaluate the complex stability under physiological conditions by incubating the complexes in 50% serum at 37 °C prior to transfection. The siRNA/PEG-DPT complexes showed comparable abilities of gene knockdown, even after co-incubation with serum for 30 min (Figure 3A). In contrast, the lipid-based RNAiFect system was significantly influenced by the serum incubation, probably due to the nonspecific association with serum proteins. Thus, these results highlighted the excellent feasibility of the PEG-DPT/siRNA complex, particularly under physiological conditions due to the segregation of siRNA into the PEG microenvironment.

The results of the endogenous gene knockdown were more fascinating. For this purpose, a cytoskeletal protein, Lamin A/C, was targeted.[1] The PEG-DPT system showed a significant gene knockdown of Lamin A/C mRNA, even after a 30-min preincubation in 50% serum, evaluated by the real-time RT-PCR analysis. Notably, in 293T cells, the expression was suppressed to the level of 20% of mock samples, which significantly exceeded the ability

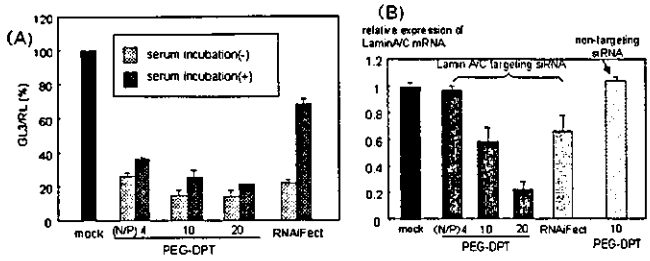

Figure 3. (A) GL3 knockdown by siRNA complexes after serum co-incubation with serum. (B) Endogenous gene (Lamin A/C) knockdown after co-incubation (n = 4; ±SD).

of the RNAiFect (Figure 3B). A similar trend was also observed in HuH-7 cells. However, neither the PEG-PLL nor PEG-DMAPA system showed any gene knockdown (data not shown). As Lamin A/C is assumed to abundantly express inside the cells, the threshold level of the siRNA's introduction that is necessary to show the inhibition of gene expression should be significantly higher than in the case of the luciferase cotransfection study. Thus, these results of PEG-DPT were very encouraging for the actual therapeutic knockdown of an endogenous gene by the siRNA delivering approach.

In conclusion, we reported here an effective siRNA nanocarrier system based on the self-assembly of the PEG-based block catiomer. The distinctive polymer design managed both a sufficient siRNA complexation and a buffering capacity of the endosomes. Notably, the siRNA/block catiomer complex revealed remarkable knockdown of the endogenous gene, even after the serum incubation. These results directed this newly designed system of block catiomer to have a promising feasibility for in vivo therapeutics.

Acknowledgment. This work was financially supported by the Core Research Program for Evolutional Science and Technology (CREST) from the Japan Science and Technology Corporation (JST) as well as by Special Coordination Funds for Promoting Science and Technology from the Ministry of Education, Culture, Sports, Science and Technology of Japan (MEXT).

Supporting Information Available: Detailed Materials and Methods section; ^{1}H NMR spectrum of PEG-DPT block copolymer (Figure S1); results of PAGE and EtBr exclusion assay of PEG-DPT (Figure S2); chemical structures of PEG-DMAPA and PEG-PLL (Figure S3); summary of EtBr exclusion assay of these copolymers (Figure S4); and result of MTT assay (Figure S5). This material is available free of charge via the Internet at http://pubs.acs.org.

References

(1) Elbashir, S. M.; Harborth, J.; Lendeckel, W.; Yalcin, A.; Weber, K.; Tuschl, T. *Nature* **2001**, *411*, 494−498.
(2) (a) Kataoka, K.; Togawa, H.; Harada, A.; Yasugi, K.; Matsumoto, T.; Katayose, S. *Macromolecules* **1996**, *29*, 8556−8557. (b) Katayose, S.; Kataoka, K. *Bioconjugate Chem.* **1997**, *8*, 702−707. (c) Vinogradov, S. V.; Bronich, T. K.; Kabanov, A. V. *Bioconjugate Chem.* **1998**, *9*, 805−812. (d) Choi, Y. H.; Liu, F.; Kim, J. S.; Choi, Y. K.; Park, J. S.; Kim, S. W. *J. Controlled Release* **1998**, *54*, 39−48. (e) Ogris, M.; Brunner, S.; Schuller, S.; Kircheis, R.; Wagner, E. *Gene Ther.* **1999**, *6*, 595−605. (f) Oupicky, D.; Konak, C.; Ulbrich, K.; Wolfert, M. A.; Seymour, L. W. *J. Controlled Release* **2000**, *65*, 149−171.
(3) Harada-Shiba, M.; Yamauchi, K.; Harada, A.; Takamisawa, I.; Shimokado, K.; Kataoka, K. *Gene Ther.* **2002**, *9*, 407−414.
(4) Itaka, K.; Yamauchi, K.; Harada, A.; Nakamura, K.; Kawaguchi, H.; Kataoka, K. *Biomaterials* **2003**, *24*, 4495−4506.
(5) Carlson, C.; Beal, P. A. *Biopolymers* **2003**, *70*, 86−102.
(6) Boussif, O.; Lezoualc'h, F.; Zanta, M. A.; Mergny, M. D.; Scherman, D.; Demeneix, B.; Behr, J. P. *Proc. Natl. Acad. Sci. U.S.A.* **1995**, *92*, 7297−7301.

JA047174R

ADVANCED MATERIALS

Reprint

Guide for Authors

Advanced Materials is an international journal that appears 24 times a year and covers all aspects of high-tech materials chemistry and physics. It publishes essays, review articles, communications, research news, letters to the editor, book reviews, interviews, materials forum, and a conference calendar, in English. No page charge is levied. Contributors should bear the interdisciplinary nature of the readership in mind, always emphasizing the importance of the topic to workers in other fields. Four copies of the manuscript plus original artwork should be sent to:

The Editorial Office
ADVANCED MATERIALS
WILEY-VCH **Tel: (+49) 6201 606 235**
Boschstraße 12 **Fax: (+49) 6201 606 500**
D-69469 Weinheim **e-mail: advmat@wiley-vch.de**
Germany

Authors of all articles will receive immediate acknowledgement of receipt of their manuscript. All contributions are subject to refereeing and/or assessment by the editors. Contributions to all sections, except Communications and Materials Forum, are usually written on invitation. Authors are welcome to submit unsolicited articles but should consult the editors as early as possible.

A diskette containing the text, references, figure captions, and tables of the manuscript should be sent to the editorial office either when the hard copy of the manuscript is submitted (Essays, Research News) or upon notification of acceptance for publication (Communications, Reviews). The version on the diskette should be the revised version, if applicable. The software and hardware used should be specified (including the number of the version of the word-processing program). Word is preferred. Please also save the text as an RTF file. Figures should be supplied in electronic form if possible (in addition to original printouts), saved using the software they were created in and also as TIF or EPS files if possible.

Reprints can be ordered when the proofs are returned to the publisher. Reprint rates are also available from the editorial office on request.

Categories of Contributions

Essays are a forum for news and opinion on topics of national and international interest. This can include, for example, news of funding and research organizations, societies, or points of controversy within materials science. Manuscripts should be 4–5 pages in length plus one display item (tables and figures). A passport-type photo and a short summary of the career to-date of the correspondence author(s) should be included.

Review Articles are peer-reviewed and give a general overview of a particular field, providing the reader with an appreciation of the importance of the work, a summary of recent developments, and a starting point in the specialist literature. Manuscripts should be between 15 and 20 pages in length and contain 9–12 display items. A passport-type photo and a short summary of the career to-date of the correspondence author(s) should be included, as well as a short abstract.

Communications are unsolicited, peer-reviewed short reports of outstanding novel findings which also have important and general implications for specialists working in other fields. The first paragraph should summarize the reasons for undertaking the work and the main conclusions that can be drawn. The final paragraph should summarize the major conclusions of the paper. Manuscripts should be up to 7 pages in length and can have up to 3 display items.

Research News Articles are intended to inform non-specialist readers of recent developments at the forefront of materials science and technology. Manuscripts should be 4–5 pages in length and can contain up to 3 display items. A short abstract should be included.

Letters to the Editor commenting on publications in *Advanced Materials* are welcome if they contribute to the scientific discussion.

Materials Forum contains short news items, correspondence, and product and conference information. Single-page manuscripts, with or without a display item, are welcome.

Book/Journal/Software Reviews are usually written on request, but suggestions are always welcome. Publishers should send relevant books to the Book Review Editor. Unsolicited books not selected for review will not be returned.

Manuscript Styling

Authors should consult articles in recent issues of the journal for examples of format.

Manuscripts should be typed, with double line spacing, on one side of the paper only. The first names, other initials, and surnames of all authors should be given, along with full postal addresses, as well as the fax number, and e-mail address of the correspondence author, who should be de signated by a star. An original and three copies of the printed manuscript are required, each accompanied by numbered artwork. Reference lists and figure legends should be submitted on separate sheets. Copies of relevant manuscripts in press or submitted elsewhere should be included, clearly marked as such.

IUPAC nomenclature should be used when naming compounds. A full guide to nomenclature and terminology can be found at the IUPAC web site www.iupac.org.

Artwork should be marked individually and clearly with the author's name and the figure number. Figures with several parts are permitted only if the parts are closely related either experimentally or logically. Suggestions can be made for cover picture designs. Photographs should be supplied as glossy prints and also in electronic format. See the guidelines to submission of graphical material for further information.

Color Artwork can be reproduced. The extra costs associated with this are expected to be met, in part, by the author. The author will be advised of the costs on acceptance of the manuscript for publication.

Tables should be subdivided by three horizontal lines only (two marking the header, one at the base). Footnotes in tables are denoted [a], [b], [c], etc.

References should be numbered sequentially as they appear in the text[1] as superscripts in square brackets.[2-5] **Only papers that are published or accepted for publication should be referenced.** The footnote option provided by many text programs should *not* be used. Journals titles should be abbreviated according to the Chemical Abstracts Service Source Index (CASSI). In citing the literature, the format below should be followed as an example:

[1] a) B. Tieke, *Adv. Mater.* **1991**, *3*, 532. b) A. R. Raju, C. N. R. Rao, *J. Chem. Soc., Chem. Commun.* **1991**, 1260.
[2] A. R. Raju, C. N. R. Rao, *J. Chem. Commun.* **1991**, 1260
[3] J. W. Grate, G. C. Frye, in *Sensors Update*, Vol. 2 (Eds: H. Baltes, W. Göpel, J. Hesse), WILEY-VCH, Weinheim **1996**, Ch. 2.
[4] B. Batlogg, "Molecular Organic Crystals", presented at *Int. Conf. on Science and Technology of Synthetic Metals 2000 (ICSM 2000)*, Bad Gastein, Austria, July 15–21, **2000.**
[5] B. R. Ezzel, W. P. Carl, W. A. Mod, *US Patent 4 330 654*, **1982.**

Note that journal and book titlees should be in italics, the year of publication in boldface type, and the volume number of journals in italics.

were used as the substrates. PFMA was prepared according to the procedure previously reported by Arai et al. [15].

Chemical Modification of the Glass Surface: The surface treatment of glass substrates was performed according to previously described procedures [16]. The individual steps are summarized briefly in the following. The substrates were ultrasonically cleaned in a washing agent (Extran MA 01, Merck Ltd.) in order to eliminate organic contamination from the surface. They were then rinsed with distilled water and dried. Next, the substrate was placed in a reaction vessel, to which was added 1 % (v/v) GPS and 0.2 % (v/v) triethylamine in anhydrous toluene. The mixture was stirred and kept at 70 °C for 4 h before washing with toluene and acetone. The substrate was then dried in a vacuum overnight at 50 °C. The obtained surface, bearing terminal epoxy groups, was hydrolyzed by immersing the substrate in a 100 mM NaCl solution adjusted to pH 4 with 10 mM HCl, heated to 70 °C for 30 min, then rinsed with distilled water and dried in a vacuum. Finally, the surface bearing terminal hydroxyl groups was immersed in a solution of 2-furoic chloride (26 mg, 0.2 mmol) in acetone (20 mL) and pyridine (23 mg, 0.3 mmol); this solution was stirred at room temperature for 24 h. It was then rinsed with distilled water and acetone and dried in a vacuum. The substrates with furan-functionalized surfaces were stored in a N_2 atmosphere.

Characterization: The molecular weight of obtained polymer, PFMA, was estimated by gel permeation chromatography with two Tosho columns (G4000HXL and G3000HXL) using tetrahydrofuran (THF) as the eluent at 40 °C after calibration with standard polystyrene. UV-visible spectroscopy (UV-3100s, Shimadzu Co.) was used to confirm the surface modification by the furan functional groups. AFM images of the sample surfaces were taken with a Nanoscope III (Digital Instruments) in a tapping mode operated under ambient conditions. The cantilever used was a commercially available etched silicon probe (TESP, Digital Instruments, Inc.) 125 μm long and with resonant frequencies of 294–356 kHz. Electrical resistivity measurements were carried out by means of a four-probe technique, using a high-performance low resistivity meter (MPC-T600, Dia Instruments Co., Ltd.).

Received: September 16, 2003
Final version: December 1, 2003

[1] M. Fuhrer, J. Nygård, L. Shih, M. Forero, Y. Yoon, M. S. C. Mazzoni, H. J. Choi, J. Ihm, S. G. Louie, A. Zettl, P. L. McEuen, *Science* **2000**, *288*, 494.
[2] N. A. Melosh, A. Boukai, F. Diana, B. Gerardot, A. Badolato, P. M. Petroff, J. R. Heath, *Science* **2003**, *300*, 112.
[3] B. Messer, J. H. Song, P. Yang, *J. Am. Chem. Soc.* **2000**, *122*, 10232.
[4] T. Rueches, K. Kim, E. Joselevich, G. Y. Tseng, C. Cheung, C. M. Lieber, *Science* **2000**, *289*, 94.
[5] a) S. Liu, R. Maoz, G. Schmid, J. Sagiv, *Nano Lett.* **2002**, *2*, 1055. b) R. Maoz, E. Frydman, S. R. Cohen, J. Sagiv, *Adv. Mater.* **2000**, *12*, 424. c) R. Maoz, E. Frydman, S. R. Cohen, J. Sagiv, *Adv. Mater.* **2000**, *12*, 725.
[6] a) Y. Huang, X. Duan, Q. Wei, C. M. Lieber, *Science* **2001**, *291*, 630. b) H. O. Jacobs, S. A. Campbell, M. G. Steward, *Adv. Mater.* **2002**, *14*, 1553. c) M. S. Sander, A. L. Prieto, R. Gronsky, T. Sands, A. M. Stacy, *Adv. Mater.* **2002**, *14*, 665. d) N. Saito, H. Haneda, T. Sekiguchi, N. Ohashi, I. Sakaguchi, K. Koumoto, *Adv. Mater.* **2002**, *14*, 418.
[7] P. Buffat, J. P. Borel, *Phys. Rev. A* **1976**, *13*, 2287.
[8] G. Schmid, *Chem. Rev.* **1972**, *92*, 1709.
[9] The surface density of furan-functionalized silane on the substrate surface was confirmed, using UV-vis spectroscopy, as ~26 Å^2/silane. This is almost the same as the calculated surface density for the occupation area of the furan moiety (~25 Å^2), which means that the functional moieties were introduced almost in a close packing on the surface.
[10] T. Oku, K. Suganuma, *Chem. Commun.* **1999**, 2355.
[11] T. Oku, K. Suganuma, *Microelectron. Eng.* **2000**, *51*, 51.
[12] S. J. Zhao, S. Q. Wang, D. Y. Cheng, H. Q. Ye, *J. Phys. Chem. B* **2001**, *105*, 12857.
[13] R. R. Couchman, *Philos. Mag. A* **1979**, *40*, 637.
[14] R. S. Berry, *Sci. Am.* **1990**, *August*, 263.
[15] H. Arai, Y. Tajima, K. Takeuchi, *Jpn. J. Appl. Phys.* **2001**, *40*, 6623.
[16] G. Jogikalmath, J. K. Stuart, A. Pungor, V. Hlady, *Colloids Surf. A* **1999**, *146*, 337.

Size-Controlled Formation of a Calcium Phosphate-Based Organic–Inorganic Hybrid Vector for Gene Delivery Using Poly(ethylene glycol)-*block*-poly(aspartic acid)**

By *Yoshinori Kakizawa*, *Kanjiro Miyata*, *Sanae Furukawa*, and *Kazunori Kataoka**

Recently, the growing interest in non-viral vector systems for in vivo gene therapy has become a strong incentive to develop a variety of advanced materials for DNA delivery with high efficiency and minimal toxicity.[1–7] Calcium phosphate (CaP)/DNA coprecipitate is one of these materials, and has been widely used for the transfection of plasmid DNA (pDNA)[8,9] and oligonucleotides (ODN)[10] into mammalian and plant cells. Nevertheless, a serious drawback of this system is that, after the initial mixing of the calcium and phosphate solutions, the growth of the CaP crystal is uncontrollably rapid, resulting in large precipitates and a steep drop in the transfection efficacy within a short period of time.[11] This uncontrollable crystal growth also causes handling and reproducibility problems. We wish to now describe a new methodology to control the calcium phosphate growth using a block copolymer with a polycarboxylate segment: poly(ethylene glycol)-*block*-poly(aspartic acid) (PEG-PAA).[12] Using PEG-PAA allows modulation of the crystal size to form a novel nanovector for pDNA with optimized transfection efficiency. The underlying concept is to prevent crystal growth through the absorption of the PAA segment of PEG-PAA on the crystal surface. This leads to the formation of core–shell particles

[*] Prof. K. Kataoka, K. Miyata
Department of Materials Science and Engineering
Graduate School of Engineering, The University of Tokyo
7-3-1 Hongo, Bunkyo-ku, Tokyo 113-8656 (Japan)
E-mail: kataoka@bmw.t.u-tokyo.ac.jp
Prof. K. Kataoka, Dr. Y. Kakizawa, S. Furukawa
Biomaterials Center, National Institute for Materials Science
1-1 Namiki, Tsukuba, Ibaraki 305-0044 (Japan)

[**] This work was supported by the Special Coordination Funds for Promoting Science and Technology from the Ministry of Education, Science, Sports and Culture, Japan (MEXT), and Core Research for Evolutional Science and Technology (CREST), the Japan Science and Technology Corporation (JST).

 DOI: 10.1002/adma.200305782

with a hybrid core of the CaP crystal and pDNA surrounded by a PEG shell. Particle properties such as size, pDNA content, and nuclease resistance of the complexed pDNA were comprehensively studied in relation to the concentration of PEG-PAA.

The effect of PEG-PAA concentration on hybrid particle formation was first investigated by a turbidity measurement based on the standard protocol of CaP/DNA coprecipitation, in which the calcium and phosphate concentrations were kept constant.[11] Figure 1 shows the time course of the change in transmittance at 350 nm after the phosphate/PEG-PAA solution was added to the calcium/DNA solution at 25 °C. In the absence of the polymer (solid line), the solution's transmittance decreased steeply in the early stage of the reaction, dropping to 60 % of the initial value within 90 s, reflecting the rapid formation of large aggregates of calcium phosphate crystals. Conversely, the increased addition of PEG-PAA from 25 to 100 $\mu g\,mL^{-1}$ progressively prevented solution turbidity and 97 % of the initial transmittance value was exceeded above a concentration of 50 $\mu g\,mL^{-1}$ of the block copolymer. These results clearly show the inhibitory effect of PEG-PAA on the growth and/or secondary aggregation of the CaP/PAA particles.

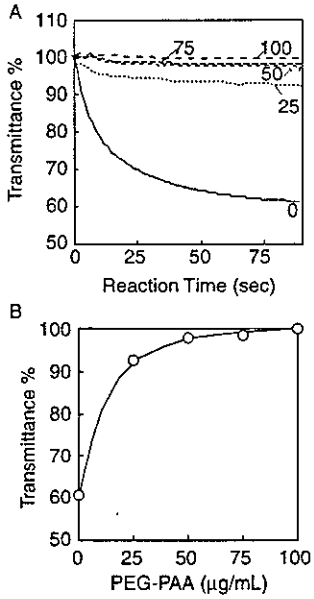

Figure 1. Effect of PEG-PAA on the growth of the calcium phosphate crystals. A) Change in the transmittance of the solutions with reaction time. Numbers denote the PEG-PAA concentration in micrograms per milliliter. B) Transmittance 90 s after mixing the solutions containing various concentrations of PEG-PAA.

The size of the hybrid particles was then evaluated using optical microscopy and dynamic light scattering (DLS) measurements. As expected, the size of the ternary hybrid particles of CaP/pDNA/PEG-PAA was found to be inversely correlated to the PEG-PAA concentration, which is consistent with the results of the turbidity measurement. Precipitates of several hundred micrometers to a few millimeters were observed by optical microscopy for the samples prepared in the concentration range of 0–25 $\mu g\,mL^{-1}$ of PEG-PAA. On the other hand, in PEG-PAA concentrations higher than 50 $\mu g\,mL^{-1}$, there is a drastic reduction in the particle diameter. Indeed, the DLS measurements revealed that the hydrodynamic diameters of the particles are progressively reduced to 3.9 μm, 320 nm, and 143 nm by increasing the PEG-PAA concentration from 50 to 75 and 100 $\mu g\,mL^{-1}$, respectively. It is obvious that the increasing amount of PEG-PAA is effective at reducing crystal size, presumably due to its adsorption on the crystal surface to compensate for the increased interfacial free energy.

The entrapping efficacy of the pDNA in the CaP/PEG-PAA hybrid particle was then determined by a centrifugation assay, in which the pDNA remaining in the supernatant after centrifugation at 15 000 rpm for 3 min was quantified by agarose gel electrophoresis. Figure 2A shows a gel image and Figure 2B the result of the densitometry analysis. At polymer concentrations lower than 25 $\mu g\,mL^{-1}$, no bands were recognizable in the gel image for pDNA, essentially indicating that all of the pDNA in the system had been incorporated into the particles. The band intensity steeply increased beyond 100 $\mu g\,mL^{-1}$, becoming constant above 150 $\mu g\,mL^{-1}$. This indicates that, above concentrations of 150 $\mu g\,mL^{-1}$ of PEG-PAA,

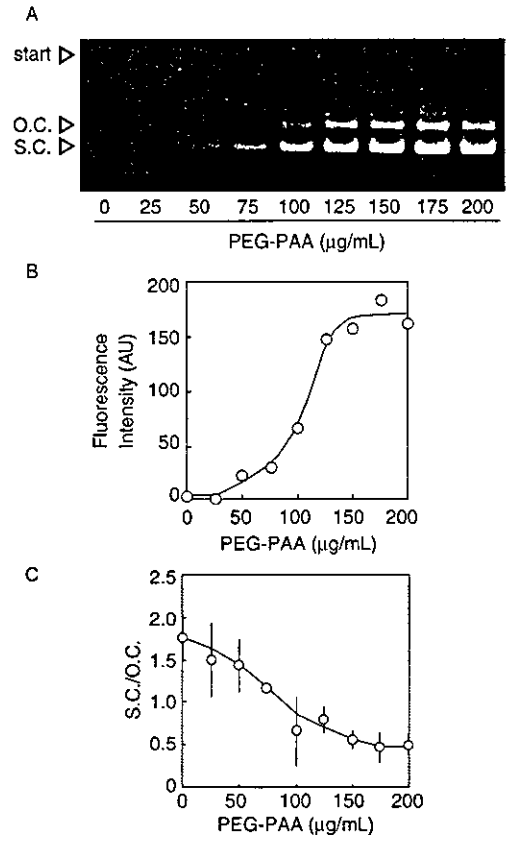

Figure 2. A,B) Centrifugation assay. A) Gel image (OC = open circular form, SC = supercoiled form of the plasmid DNA); B) densitometry analysis of the gel image. C) Enzyme protection assay. Error bars represent the standard deviation derived from triplicate experiments.

the pDNA was almost excluded from the particles. The decrease in the bound pDNA with increasing PEG-PAA concentration suggests that PEG-PAA and pDNA bind competitively to the calcium phosphate, and the exclusion of pDNA from the complex occurs at a higher polymer concentration, because the PAA segment itself may act as a nucleator or tying molecule during the formation of the complexes.[13,14]

Nuclease resistance of the pDNA associated with the CaP/PEG-PAA particles was then investigated using an endonuclease, deoxyribonuclease I (Dnase I). The metabolite of the pDNA was visualized by gel electrophoresis and the fluorescence intensity of the bands corresponding to the supercoiled (SC) and open circular (OC) forms was determined by densitometry analysis. The ratio of the fluorescence intensity of the SC, a native form, to the OC, a nicked form, was used as an index to quantitatively evaluate the degree of nuclease digestion as a function of the PEG-PAA concentration (Fig. 2C). Fluorescence intensity ratios for the naked pDNA before and after enzyme treatment were 3.26 ± 0.21 and 0.28 ± 0.12, respectively. Compared to the naked pDNA, degradation was significantly suppressed through association with CaP/PEG-PAA hybrid particles, particularly at lower polymer concentrations. In line with the trend in the inclusion efficacy of the pDNA into the hybrid particles seen in Figures 2A,B, the nuclease resistance substantially increased with decreasing polymer concentration.

Worth noting is the transfection activity of the hybrid particles to 293 cells evaluated at various concentrations of the PEG-PAA in the absence of fetal calf serum (FCS). As shown in Figure 3, the expression of the luciferase gene peaked at a polymer concentration of 50 $\mu g\,mL^{-1}$—six to seven times higher than with calcium phosphate alone (0 $\mu g\,mL^{-1}$). A similar trend in the activity–concentration profile was observed in the presence of FCS with a slightly lower expression than in the absence of FCS. Transfection experiments using HeLa cells showed a similar profile (data not shown), suggesting that the phenomenon is caused by the propensities of the vector itself. The improvement in the gene expression with an increase in the PEG-PAA concentration from 25 to 50 $\mu g\,mL^{-1}$ is significant, even though the entrapment efficacy and the enzyme tolerability of the pDNA in this concentration range are comparable (see Fig. 2). Presumably, the abrupt size reduction of the hybrid particles within this concentration range may play a substantial role in the steep increase in the transfection efficacy through the possible enhancement of their cellular internalization by endocytosis. Note that an enhancement of gene expression accompanied by the size reduction was reported for other synthetic vector systems composed of cationic polymers.[15,16] On the other hand, a gradual decrease in the expression level above 50 $\mu g\,mL^{-1}$ of the PEG-PAA may reasonably be due to the decreased entrapment efficacy of the pDNA in the hybrid particles.

In the calcium phosphate method, the control of the crystal size is the critical issue in obtaining a higher transfection efficacy. We demonstrated that the transfection efficacy of the CaP/pDNA system can be maximized via modulation of the particle size using a block copolymer. The advantage of the hybrid system is that the calcium phosphate core of the particles serves as a low-toxicity nanocontainer for the DNA, and the versatility of the chemical structure of the block copolymer may even allow the incorporation of functional molecules, such as the specific ligands for the cellular uptake on the distal end of the shell-forming segments.[17] It should be noted that the cytotoxicity of the hybrid particles in the PEG-PAA concentration range from 0 to 200 $\mu g\,mL^{-1}$ was indeed negligible (data not shown). With these desirable characteristics, calcium phosphate-based hybrid vectors might find wide in vivo applications as gene and other nucleic acid-based delivery systems with an appreciable biocompatibility.

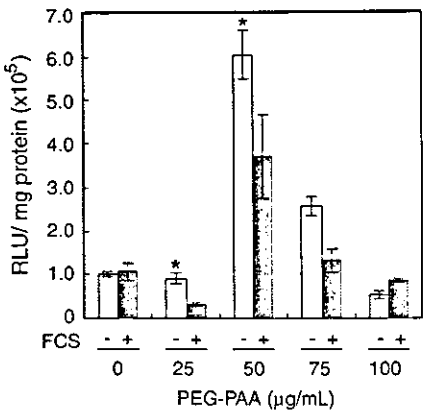

Figure 3. Effect of PEG-PAA concentration on the reporter gene expression. Samples were incubated with 293 cells in the absence (open bars) or presence (shaded bars) of 10% FCS. Results are expressed as RLU mg^{-1} of protein determined by BCA protein assay. Error bars represent standard error of the mean derived from triplicate transfection experiments. The symbol * indicates the statistical significance in the transfection levels ($p < 0.01$) between 25 and 50 $\mu g\,mL^{-1}$ of the PEG-PAA.

Experimental

Chemicals: Poly(ethylene glycol)-*block*-poly(aspartic acid) (PEG-PAA) was synthesized as previously described [12]. The molecular weight of the PEG segment was 12 000 and the degree of polymerization of the PAA segment was 24. The plasmid pGL3 control luciferase reporter vector (Promega) was amplified with a competent *Escherichia coli* strain JM 109 and purified with a high-speed purification kit (Qiagen). The Dnase I solution was purchased from Takara Shuzo Co. All other reagents were used as received.

Preparation of Hybrid Vectors: pDNA dissolved in a 10 mM tris(hydroxymethyl)aminomethane-ethylene diamine-*N,N,N′,N′*-tetraacetic acid solution (tris-EDTA) buffer (pH 7.4) was diluted with water and supplemented with a 2.5 M $CaCl_2$ solution to obtain a 2 × calcium/pDNA solution (pDNA 50 $\mu g\,mL^{-1}$, $CaCl_2$ 250 mM). The block copolymer, PEG-PAA, was dissolved in the phosphate solution (1.5 mM Na_2HPO_4, 50 mM *N*-2-hydroxyethylpiperazine-*N′*-2-ethanesulfonic acid (HEPES), 140 mM NaCl, pH 7.1) to obtain a 2 × phosphate/PEG-PAA solution (polymer concentration 0–400 $\mu g\,mL^{-1}$). One volume of the 2 × phosphate/PEG-PAA solution was added to an equal volume of the 2 × calcium/pDNA solution (final concentrations; pDNA 25 $\mu g\,mL^{-1}$, calcium ions 125 mM, phosphate ions 0.75 mM). After mixing with a vortex mixer for 3 s, the solutions were incubated at 25 °C for 24 h unless otherwise stated.

Turbidity Measurements: 2 × calcium/pDNA and 2 × phosphate/PEG-PAA solutions (1 mL) preincubated at 25 °C were directly mixed in a polystyrene cuvette. The transmittance at 350 nm was then measured for 90 s with continuous stirring at 1000 rpm at 25 °C.

Centrifugation Assays: Sample solutions (100 μL) prepared at polymer concentrations ranging from 0 to 200 μg mL^{-1} were incubated for 24 h at 25 °C and centrifuged at 15 000 rpm for 3 min. The supernatant (20 μL) from each sample was recovered and applied to gel electrophoresis in order to determine the amount of the pDNA. Gel electrophoresis was conducted using a 0.9 % agarose gel and 40 mM tris-acetate buffer (10 mM EDTA). Images of the gels stained with ethidium bromide were acquired and analyzed using an ImageMaster-CL (Amersham Biosciences).

Enzyme Protection Assays: Dnase I solution (25 μL, 0.001 U μL^{-1}) was added to the complex solution (100 μL) and incubated for 1 h at 37 °C. An aliquot (25 μL) was withdrawn from the reaction mixture and 25 μL of a saturated EDTA solution was immediately added to stop the enzyme reaction. Samples were applied to gel electrophoresis and analyzed as described in the centrifugation assay.

Evaluation of Size of Complexes: The size of the particles formed at high polymer concentrations was determined by DLS as described in detail elsewhere [12]. The DLS measurements were carried out using a DLS-7000 instrument (Otsuka Electronics Co.). Vertically polarized light with a wavelength of 488 nm from an Ar-ion laser (15 mW) was used as the incident beam. All measurements were conducted at 25 °C, and data were analyzed by the cumulant method to determine the hydrodynamic diameters of the particles. Precipitates formed at low polymer concentrations were observed by light microscopy (Axiovert 200, Carl Zeiss Co.).

Transfection Experiments: 293 and HeLa cells were respectively grown in Dulbecco's modified Eagles medium (DMEM) supplemented with 10 % FCS at 37 °C in a 5 % CO_2 humidified atmosphere. After 24 h of incubation in six-well culture plates, the cells were rinsed with serum-free DMEM and 1000 μL of culture medium with or without FCS was added to each well. Immediately before the transfection, the particle solutions were suspended by pipetting and 100 μL was added to each well. After 6 h of incubation, the medium was replaced with fresh medium containing 10 % FCS. Cells were incubated for an additional 24 h in the complete medium. A luciferase assay was conducted with a luminometer (Fluoroskan Ascent FL, Labsystems) using a Promega kit according to the manufacturer's protocol. Results were expressed as relative light units (RLU) per milligram of protein determined using a BCA protein assay kit (Pierce; BCA = bicinchoninic acid). The error bars represent standard error of mean derived from the triplicate transfection experiments.

Cytotoxicity Assays: 293 and HeLa cells were used for the cytotoxicity assay. Cells were plated in 96-well plates at a density of 10 000 cells per well and allowed to adhere overnight. The hybrid particles, formed at the varying polymer concentrations from 0 to 200 μg mL^{-1} were added as suspension in the medium to the semiconfluent cellular monolayer in the presence of 10 % FCS, and incubated for 24 h at 37 °C. Subsequently, the cell viability was determined by a 3-(4,5-dimethylthiazol-2-yl)-2,5-diphenyltetrazolium bromide (MTT) assay.

Received: August 2, 2003
Final version: January 5, 2004

[1] *Self-Assembling Complexes for Gene Delivery* (Eds: A. V. Kabanov, P. L. Felgner, L. W. Seymour), John Wiley, Chichester, UK **1998**.
[2] D. Luo, W. M. Saltzman, *Nat. Biotechnol.* **2000**, *18*, 33.
[3] A. Akinc, D. M. Lynn, D. G. Anderson, R. Langer, *J. Am. Chem. Soc.* **2003**, *125*, 5316.
[4] O. Boussif, F. Lezoualch, M. A. Zanta, M. D. Mergny, D. Ssherman, B. Demeneix, J. P. Behr, *Proc. Natl. Acad. Sci. USA* **1995**, *52*, 7297.
[5] M. Cotten, F. Langlerouault, H. Kirlappos, E. Wagner, K. Mechtler, M. Zenke, H. Beug, M. L. Birnstiel, *Proc. Natl. Acad. Sci. USA* **1990**, *87*, 4033.
[6] Y. Kakzizawa, K. Kataoka, *Adv. Drug Delivery Rev.* **2002**, *54*, 223.
[7] S. Katayose, K. Kataoka, *Bioconjugate Chem.* **1997**, *8*, 702.
[8] F. L. Graham, A. J. van der Eb, *Virology* **1997**, *52*, 456.
[9] C. Chen, H. Okayama, *Mol. Cell. Biol.* **1987**, *7*, 2745.
[10] H. Tolou, *Anal. Biochem.* **1993**, *215*, 156.
[11] M. Jordan, A. Schallhorn, F. M. Wurm, *Nucleic Acids Res.* **1996**, *624*, 596.
[12] Y. Kakizawa, K. Kataoka, *Langmuir* **2002**, *12*, 4539.
[13] J. V. Gracia-Ramas, P. Carmona, A. Hidalgo, *J. Colloid Interface Sci.* **1981**, *83*, 479.
[14] S. I. Stupp, G. W. Ciegler, *J. Biomed. Mater. Res.* **1992**, *26*, 169.
[15] C. L. Gebhart, S. Sriadibhatla, S. Vinogradov, P. Lemieux, V. Alakhov, A. V. Kabanov, *Bioconjugate Chem.* **2002**, *13*, 937.
[16] E. Wagner, M. Cotten, R. Foisner, M. L. Birnstiel, *Proc. Natl. Acad. Sci. USA* **1991**, *88*, 4255.
[17] K. Kataoka, A. Harada, D. Wakebayashi, Y. Nagasaki, *Macromolecules* **1999**, *32*, 6892.

Growth of Silicon Oxide in Thin Film Block Copolymer Scaffolds**

By *Dong Ha Kim*, *Xinqiao Jia*, *Zhiqun Lin*, *Kathryn W. Guarini*, and *Thomas P. Russell**

Numerous fabrication methods have been reported to generate surfaces patterned with regularly sized and spaced features on the nanometer-scale. Due to their ability to self-assemble into a variety of ordered nanoscale morphologies, block copolymers offer an attractive route to overcome the limitations of conventional lithographic techniques.[1–11] Silicon dioxide has tremendous promise for applications ranging from microelectronic to photonic devices, and significant efforts have been made to fabricate tailored structures.[12–16] Combining the self-assembly of blocks with the synthesis of silicon oxide may offer a unique approach to device fabrication.

[*] Prof. T. P. Russell, Dr. D. H. Kim,[+] Dr. X. Jia,[++] Dr. Z. Lin[+++]
Silvio O. Conte National Center for Polymer Research
Polymer Science and Engineering Department
University of Massachusetts at Amherst
Amherst, MA 01003 (USA)
E-mail: russell@mail.pse.umass.edu
K. W. Guarini
IBM T. J. Watson Research Center
Yorktown Heights, NY 10598 (USA)
[+] Current address: Max Planck Institute for Polymer Research, Ackermannweg 10, D55128 Mainz, Germany.
[++] Current address: Department of Chemical Engineering, Massachusetts Institute of Technology, Cambridge, MA 02139, USA.
[+++] Current address: Department of Materials Science and Engineering, University of Illinois at Urbana-Champaign, Urbana, IL 61801, USA.
[**] We are grateful for the financial support of the Department of Energy, Basic Energy Sciences under contract DE-FG02-96ER45612, National Science Foundation under the partnership in Nanotechnology (CTR-9871782), and NSF-sponsored Material Research Science and Engineering Center at the University of Massachusetts at Amherst.

  DOI: 10.1002/adma.200404906